UPMC PARIS UNIVERSITAS

*B. Bellier*

# Master BMC
# Immunologie Fondamentale

## Activation lymphocytaire T

**Bertrand Bellier**
UPMC CNRS UMR7087
Biologie et Thérapeutique des Pathologies Immunitaires
Pitié-Salpétrière - Paris - France
bertrand.bellier@upmc.fr

UPMC PARIS UNIVERSITAS

B. Bellier

# Activation lymphocytaire T

- **Le rapprochement cellulaire**
- **La synapse immunologique (BMC 403)**
- **Les molécules de l'activation**
  - TCR: CMH-Ag + Co-récepteur CD4, CD8
  - Mol co-stimulation
  - Cytokines

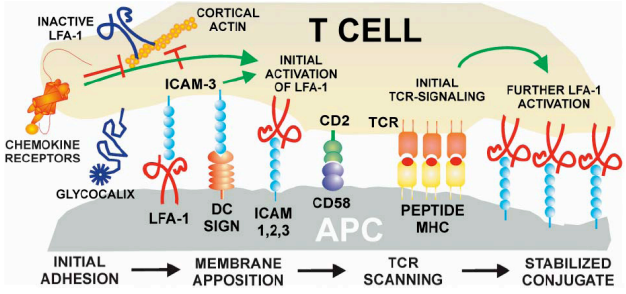


**Fig. 1. Sequence of interaction and redistribution of cell surface molecules during initial immune adhesive contact.** The initial adhesive contact is mediated by ICAM-3 interaction with APC ligands (LFA-1, or DC-SIGN). ICAM-3 activation and chemokine receptor signaling induce redistribution of cortical actin and initial activation of LFA-1, leading to membrane apposition that allows CD2–CD58 interactions and TCR searching of MHC-peptide. Signaling by TCR, CD2 and ICAM-3 contributes to further LFA-1 activation that leads to the stabilization of the conjugate.

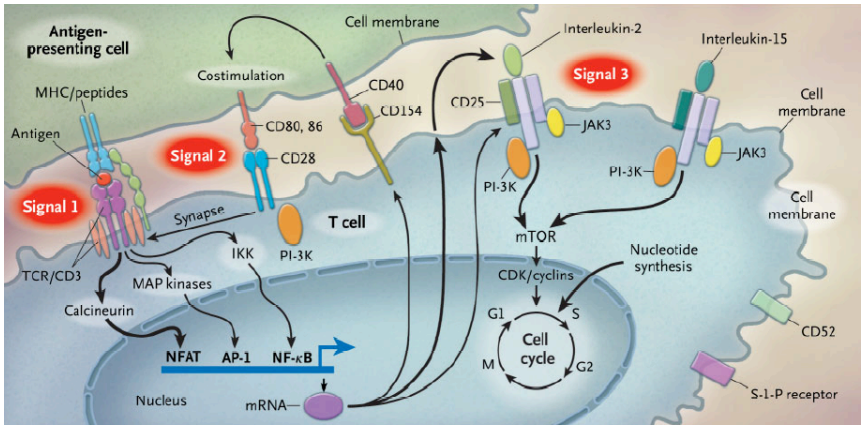


- **Aspects quantitatifs et qualitatifs de l'activation**
  - Affinité de l'interaction
  - Avidité de l'interaction
  - Dynamique des interactions moléculaires
- **et ses conséquences sur le développement de la réponse immunitaire**
  - Détermine le programme de différenciation T

B. Bellier

# Bases moléculaires de la reconnaissance antigénique

## Influence des paramètres de l'interaction TCR/CMH-Ag

# Reconnaissance antigénique

**Interactions TCR/ MHC-Ag:**

**< Vert = MHC**
**Rouge = TCR**
**Jaune = peptide antigénique**

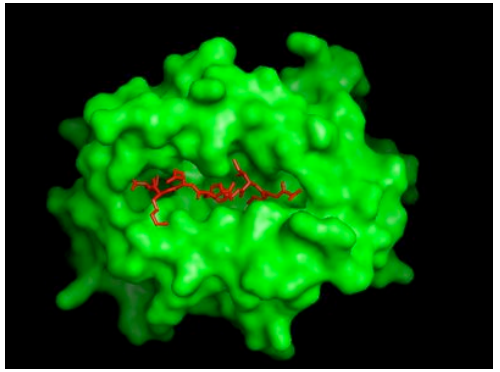

Affinité TCR /CMH-Ag: **KD ~1-50 µM.**

Significativement plus faible que les autres interactions protéines-protéines aux conséquences biologiques

UPMC PARIS UNIVERSITAS

B. Bellier

# Affinité des TCR
# TCR/CMH-I vs TCR/CMH-II

**Human TCR-Binding Affinity Is Governed by MHC Class Restriction**[1]

David K. Cole,*‡ Nicholas J. Pumphrey,† Jonathan M. Boulter,‡ Malkit Sami,† John I. Bell,* Emma Gostick,* David A. Price,* George F. Gao,*§ Andrew K. Sewell,*‡ and Bent K. Jakobsen[2†]

*J. I. 2007*

Table IV. *Kinetic data at 25°C*[a]

| | $K_{on}$ $M^{-1}s^{-1}$ | $K_{off}$ $s^{-1}$ | $K_D$ μM ($K_{off}/K_{on}$) |
|---|---|---|---|
| TCR-I/pMHC-I | | | |
| gp100 TCR/A2 gp100 | $3.1 \times 10^4$ | 0.23 | 7 |
| TEL TCR/A2 Tel | $3.5 \times 10^3$ | 0.14 | 40 |
| LC13 TCR/B8 EBNA | $8.7 \times 10^4$ | 0.63 | 7 |
| AM3 TCR/A24 EBV | $7.3 \times 10^3$ | 0.21 | 28 |
| JM22 TCR/A2 Flu | $3.2 \times 10^4$ | 0.15 | 5 |
| A6 TCR/A2 Tax | $2.9 \times 10^4$ | 0.10 | 4 |
| GRB TCR/B27 Flu | $3.9 \times 10^4$ | 0.09 | 3 |
| MEL TCR/A2 Mel | $>1 \times 10^6$ | >1 | nm |
| TCR-II/pMHC-II | | | |
| MAW13 TCR/DR3 M-HSP | $4.0 \times 10^3$ | 0.12 | 30 |
| AH1.23 TCR/DR4 C-HSP | $4.4 \times 10^3$ | 0.16 | 36 |
| 1A12 TCR/DR2 MBP | $2.1 \times 10^3$ | 0.17 | 81 |
| 2E11 TCR/DR2 MBP | $5.9 \times 10^3$ | 0.73 | 123 |
| HA1.7 TCR/DR1 HA | $>1 \times 10^6$ | >1 | nm |
| HA1.7 TCR/DR4 HA | $>1 \times 10^6$ | >1 | nm |
| Average TCR-I/pMHC-I | $3.3 \times 10^4 \pm 2.9 \times 10^4$ | 0.22 ± 0.19 | 13 ± 15 |
| Average TCR-II/pMHC-II | $4.1 \times 10^3 \pm 1.3 \times 10^3$ | 0.30 ± 0.29 | 68 ± 43 |

[a] nm, Not measurable, i.e. the kinetics were too fast to accurately determine.

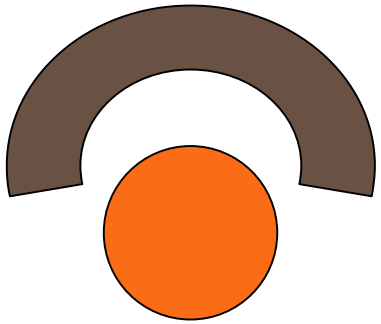

**Ka= Kon/Koff**
**Kd= 1/Ka**

**Kon: Taux d'association**
**Koff: Taux de dissociation**

- human TCRs bind to pMHC-I with approximately **five times greater** affinity than to pMHC-II.
- **faster on-rates** for TCR-I, compared to TCR-II, are indicative of a higher degree of conformational flexibility and higher entropic cost upon binding for the TCR-II interactions.
- Koff is a measure of the stability of a protein-protein interaction. no significant difference between the average **Koff** value for TCR binding to pMHC-I or pMHC-II. This observation is supported by TCR/pMHC complex crystal structures, which show that the **number of molecular contacts is relatively conserved** for TCR-I and II binding

UPMC PARIS UNIVERSITAS

B. Bellier

# Engagement du TCR: Rôle du CDR
# Définit l'affinité pour pCMH

Hb peptide

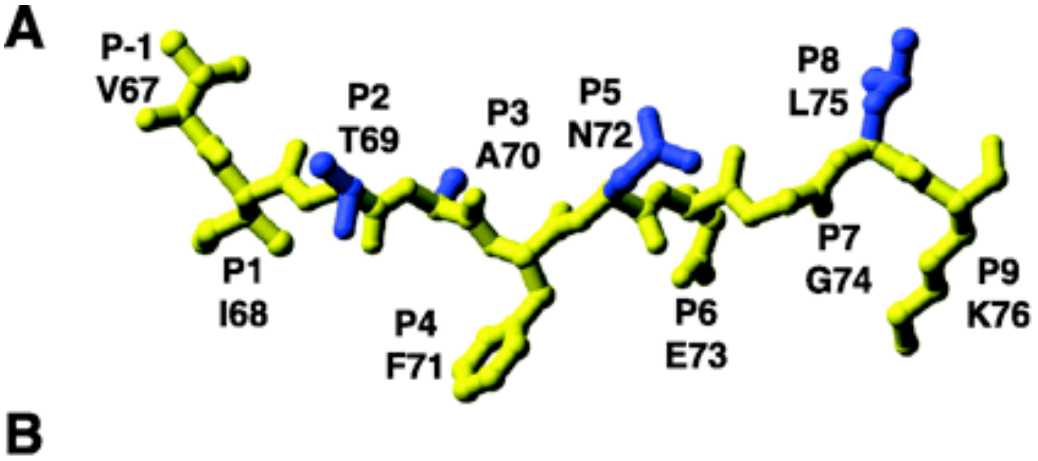


B

TCR mutants

| T cell | CDR mutations β:1 2 3 α:1 2 3 | $K_D$ ($k_{off}/k_{on}$) *nM* | Half-Life *s* | $k_{on}$ $M^{-1}s^{-1}$ | $k_{off}$ $s^{-1}$ |
|---|---|---|---|---|---|
| M1 | ○○○ ○○○ | 19,860 ± 3,630 | 6.8 ± 0.7 | 5,220 ± 410 | 0.1023 ± 0.0107 |
| M4 | ○○○ ○○● | 580 ± 185 | 28.5 ± 0.8 | 42,670 ± 17,430 | 0.0243 ± 0.0007 |
| M14 | ○○● ○○● | 81 ± 2 | 48.9 ± 2.4 | 173,500 ± 3,500 | 0.0141 ± 0.0007 |
| M15 | ○○● ●○● | 25 ± 5 | 104.4 ± 9.1 | 281,500 ± 34,800 | 0.0068 ± 0.0006 |

Aff >
KD <
Koff <
Kon >

Hb peptide residues and location of CDR mutations in high-affinity 3.L2 TCR mutants. **A**, Structure of Hb peptide (ITAFNEGLK) showing in blue the location of the four surface-exposed residues P2(T), P3(A), P5(N), and P8(L). **B**, 3.L2 M1 (unmutated CDRs) and **three higher affinity mutants** (M4, M14, and M15) with the location of their CDR mutations and respective KD, t1/2, kon, and koff values (43 ). The CDRbeta1,2,3 and CDR{alpha}1,2,3 are designated from left to right by circles: {circ}, indicate that the CDR is not mutated; •, indicate mutations in the CDRbeta or CDR{alpha}, respectively. The amino acid mutations in these regions are the same as previously published (43 ).

UPMC PARIS UNIVERSITAS
B. Bellier

# Engagement du TCR: Rôle du peptide Agoniste, Agonsite Partiel, Antagoniste

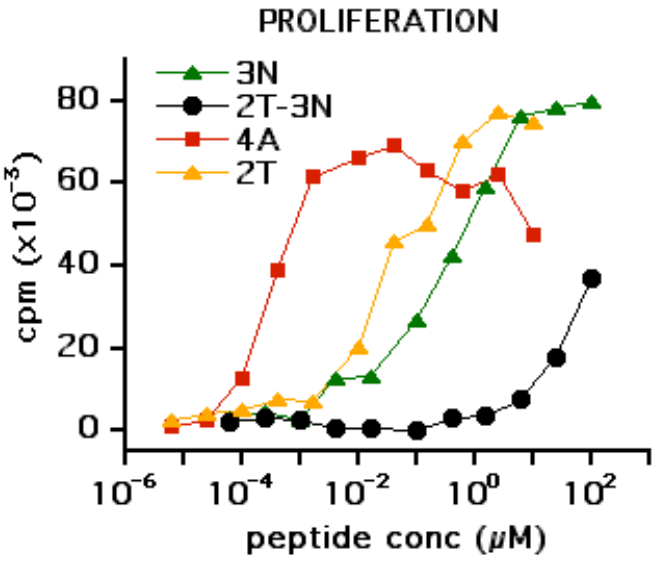


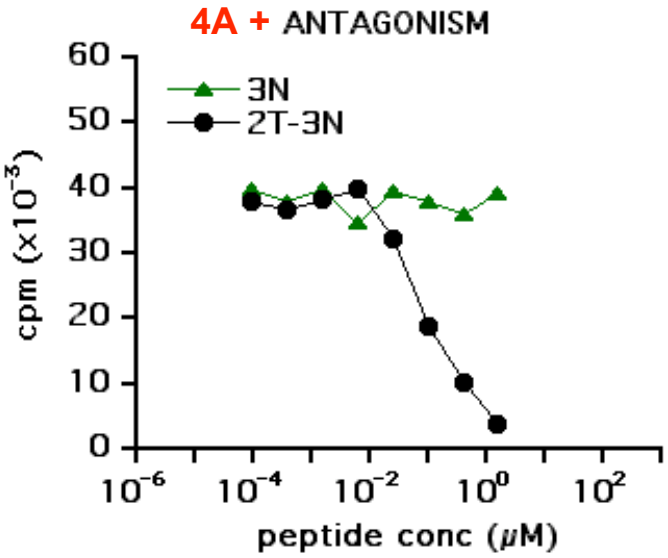


Altered MBP 1-11 Peptides are **Partial Agonists**

Agonist = 4A

Substitution of the Gln-3 residue, a TCR contact, with Asn (3N) diminishes the ability of the peptide to stimulate T-cell proliferation (top). Substitution of the Ser-2 residue, an MHC contact, with Thr (2T) also diminishes the ability of the peptide to stimulate T-cell proliferation (top). When combined, these two mutations (2T-3N), profoundly diminishes the peptide activity. Molecular models suggested that the 2T substitution would alter the side-chain conformation of the 3N residue. **Although the 2T-3N peptide does stimulate T-cell proliferation at high concentrations (top), at lower concentrations it blocks proliferation induced by the agonist 4A peptide.** These partial agonist peptides have the ability to modulate T-cell responses and may be useful in the treatment of autoimmune diseases.

In the bottom panel, antigen presenting cells were pre-pulsed with the A4 peptide and then added to T cells with altered peptide.
Proliferation was measured as the incorporation of tritiated thymidine.

**>> Cas de l'échappement viral**

# Interaction TCR/CMH-Ag:
# Présentation / Reconnaissance

anchor

recognition

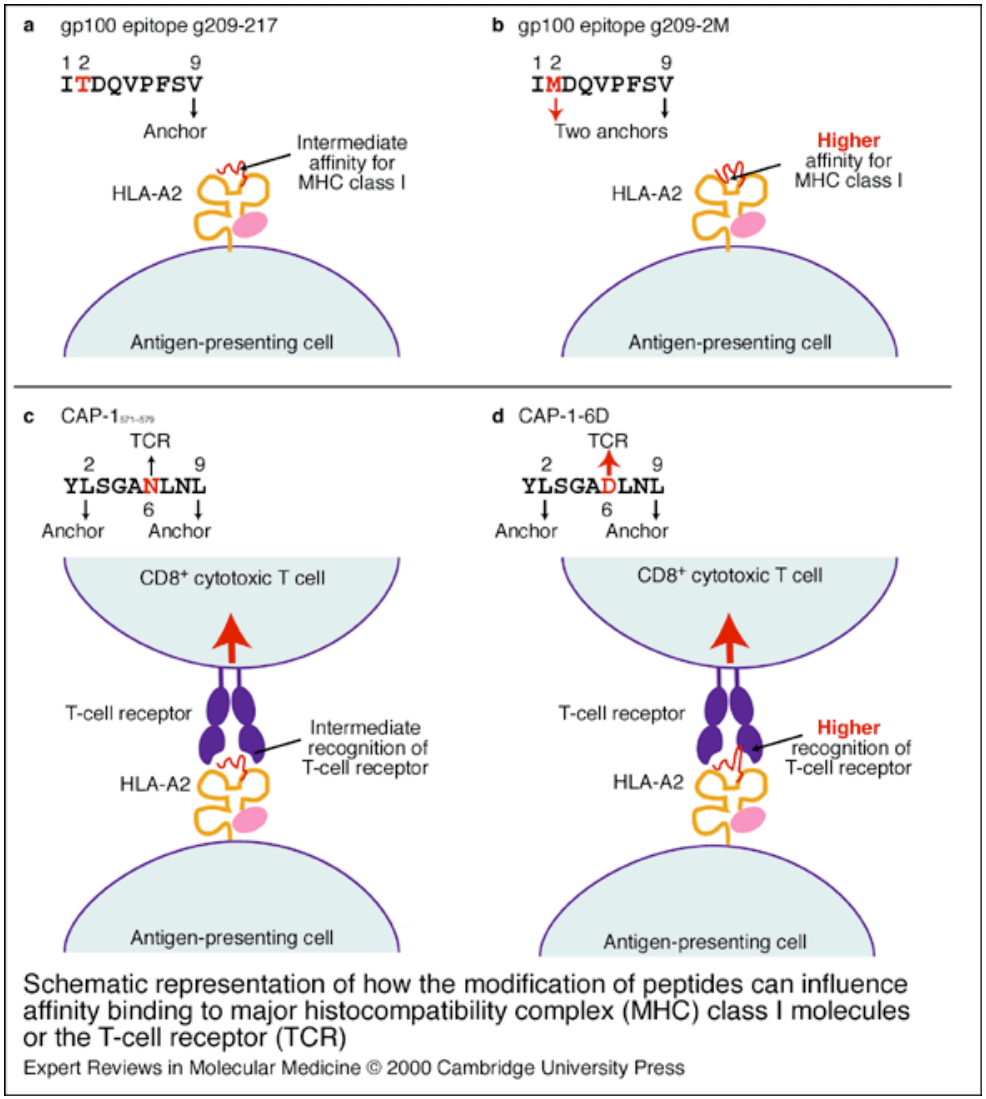


Schematic representation of how the modification of peptides can influence affinity binding to major histocompatibility complex (MHC) class I molecules or the T-cell receptor (TCR)



Schematic representation of how the **modification of peptides can influence affinity binding to major histocompatibility complex (MHC) class I molecules or the T-cell receptor (TCR).** (a) Substitution of a (**potential anchor**) residue (the second amino acid in this case) in the gp100 epitope g209-217 (ITDQVPFSV). Replacing a threonine residue (T) with a methionine residue (M) results in the modified g209-2M peptide (IMDQVPFSV). (b) This change alters the **binding affinity of the peptide to the HLA-A2** molecule, increasing the affinity of the peptide for the MHC (because of its second anchor position for the MHC), and stabilising the complex (Refs 45, 90). This leads to an increased recognition of the MHC-peptide complex by the TCR. (c) Substitution of an amino acid residue that is not an anchor for MHC can, instead, **alter the recognition of MHC-bound peptide for the TCR**. For example, replacing an asparagine residue (N) at position 6 of the CAP-1571-579 peptide (YLSGANLNL) with an aspartic acid residue (D) results in the modified CAP-1-6D peptide (YLSGADLNL). (d) This modification does not alter the binding affinity of the peptide to the HLA-A2 molecule, but rather **increases the recognition** of the MHC-peptide complex by the TCR

*Heidi Hörig; Expert Reviews in Molecular Medicine, 2000*

UPMC PARIS UNIVERSITAS

B. Bellier

# Importance de l'affinité du TCR pour l'activation lymphocytaire (1)

## CD8$^+$ T Cell Activation Is Governed by TCR-Peptide/MHC Affinity, Not Dissociation Rate[1]

Shaomin Tian,* Robert Maile,*† Edward J. Collins,*‡ and Jeffrey A. Frelinger[2]*

**CD8+ TCR-transgénique (P14 = TCR Va2 Vb8)**
**Ag = GP33-41 / LCMV**
**Or GP33-41 mutants (C9L, K1MC9M)**

Table I. *Peptide variants of gp33*

| Mutation Site | Sequence | Peptide Mutant |
|---|---|---|
| None | KAVYNFATC | gp33 |
| P1 | KAVYNFATC | K1A, K1D, K1E, K1F, K1L, K1N, K1R, K1S, K1V, K1W, K1Y |
| P2 | KAVYNFATC | A2D, A2E, A2F, A2G, A2K, A2L, A2N, A2R, A2S, A2T, A2V, A2W, A2Y |
| P3 | KAVYNFATC | V3A, V3D, V3E, V3F, V3G, V3K, V3L, V3N, V3R, V3S, V3T, V3W, V3Y |
| P4 | KAVYNFATC | Y4A, Y4C |
| P6 | KAVYNFATC | F6L |
| P9 | KAVYNFATC | C9A, C9D, C9E, C9F, C9K, C9L, C9M, C9N, C9R, C9S, C9V, C9W |
| P1, P9 | KAVYNFATC | K1AC9M, K1MC9M, K1SC9M |
| P3, P9 | KAVYNFATC | V3LC9M |
| P4, P9 | KAVYNFATC | Y4FC9M, Y4SC9M |

Table II. *Effects of gp33 variants on T cell cytotoxicity, IFN-γ production, and TCR binding*

| Peptide | $EC_{50}^{CTL}$ (nM)[a] | $EC_{50}^{IFN}$ (μM)[b] | $K_D$ (μM)[c] | $\Delta G$ (kcal · mol$^{-1}$)[d] | $k_{on}$ ($\times 10^5$ M$^{-1}$ · s$^{-1}$)[e] | $k_{off}$ (s$^{-1}$)[e] | $t_{1/2}$ (s)[f] |
|---|---|---|---|---|---|---|---|
| gp33 | 16.8 ± 16.8 | 0.06 ± 0.01 | 12.2 ± 2.2 | −6.79 | 1.33 ± 0.27 | 1.35 ± 0.68 | 0.51 |
| C9F | 0.53 ± 0.36 | 0.56 ± 0.44 | 9.4 ± 0.5 | −6.95 | 1.19 ± 0.01 | 1.15 ± 0.01 | 0.60 |
| C9L | 1.36 ± 2.1 | 0.47 ± 0.63 | 8.6 ± 0.2 | −7.00 | 0.89 ± 0.02 | 0.79 ± 0.02 | 0.88 |
| C9M | 1.59 ± 2.67 | 0.92 ± 0.39 | 9.1 ± 1.4 | −6.96 | 1.42 ± 0.54 | 1.2 ± 0.46 | 0.58 |
| C9V | 3.20 ± 5.60 | 1.23 ± 0.27 | 10.8 ± 0.3 | −6.86 | 1.16 ± 0.03 | 1.25 ± 0.03 | 0.55 |
| K1MC9M | 8.58 ± 5.27 | 0.13 ± 0.09 | 74.5 ± 13.6 | −5.70 | 0.33 ± 0.08 | 3.53 ± 0.7 | 0.20 |
| K1R | 49.0 ± 22.0 | 7.96 ± 1.06 | 81.6 ± 10.6 | −5.65 | 1.31 ± 0.47 | 10.6 ± 3.5 | 0.065 |
| K1SC9M | >50,000 | 28.0 ± 4.55 | 267 | −4.94 | 0.01 | 0.26[g] | 2.67 |
| V3LC9M | >50,000 | 112.8 ± 75.3 | 264 ± 103[g] | −4.94 | ND[g] | ND[g] | ND[g] |
| Y4A | 8,870 ± 5,550 | 11.57 ± 7.47 | 63.0 ± 14.3 | −5.8 | 0.38 ± 0.07 | 2.2 ± 0.57 | 0.32 |
| Y4FC9M | >50,000 | 38.55 ± 22.03 | 681[g] | −4.38 | ND[g] | ND[g] | ND[g] |
| Y4SC9M | >50,000 | 264.1 ± 157.5 | 530[g] | −4.53 | ND[g] | ND[g] | ND[g] |

[a] $EC_{50}^{CTL}$ is the effective concentration of peptide that gives 50% maximum CTL activity as determined by 4-h chromium release assay. The values represent the mean ± SD of three to five experiments.
[b] $EC_{50}^{IFN}$ is the effective concentration of peptide that induces 50% of the maximum amount of IFN-γ as determined by ELISA. The values represent the mean ± SD of three to four experiments.
[c] Determined from steady-state SPR data with software Scrubber. The values represent the mean ± SD of two to three experiments.
[d] Determined by $\Delta G = -RT \ln K_D$, where RT at 25°C is −0.6 kcal · mol$^{-1}$.
[e] Determined from kinetic SPR data with software CLAMP XP. The values represent the mean ± SD of two to three experiments.
[f] Half-life of dissociation of pMHC from P14 TCR. Determined by $t_{1/2} = \ln 2/k_{off}$.
[g] From Tissot et al. (42); ND, determined.
[h] Derived from $k_{off} = K_D \times k_{on}$.

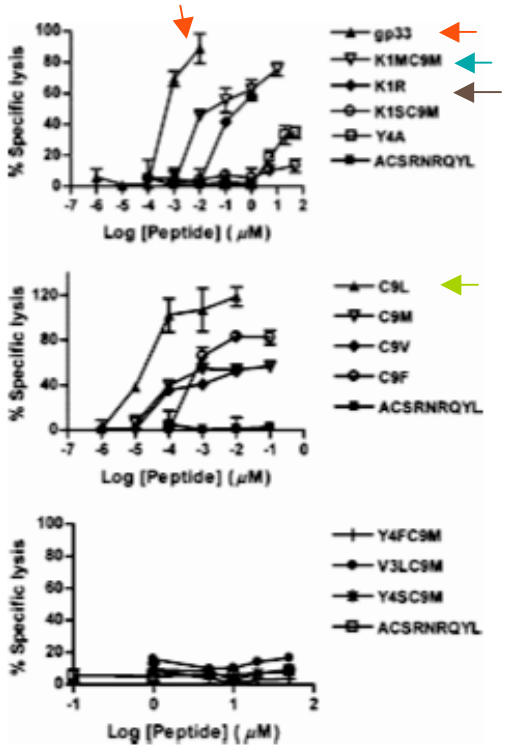


**FIGURE 3.** Viral epitope gp33 and APLs variably sensitize P14 T cells to kill target cells. EL4 cells labeled with $^{51}Cr$ and pulsed with peptides at various concentrations were incubated with activated splenocytes from P14 TCR transgenic mice (E:T ratio = 5) for 4 h. Specific lysis of EL4 cells was measured by $^{51}Cr$ release. Irrelevant HY(K1A) peptide (ACSRN RQYL) was used as negative control. Data are shown as mean ± SD ($n$ = 3), and are representative of three to five independent experiments. Using GraphPad Prism, data were fit into sigmoidal dose-response model to obtain $EC_{50}^{CTL}$ values (shown in Table II) (fitting curves are not shown).

T-

# Importance de l'affinité du TCR pour l'activation lymphocytaire (2)

CTL IFNg

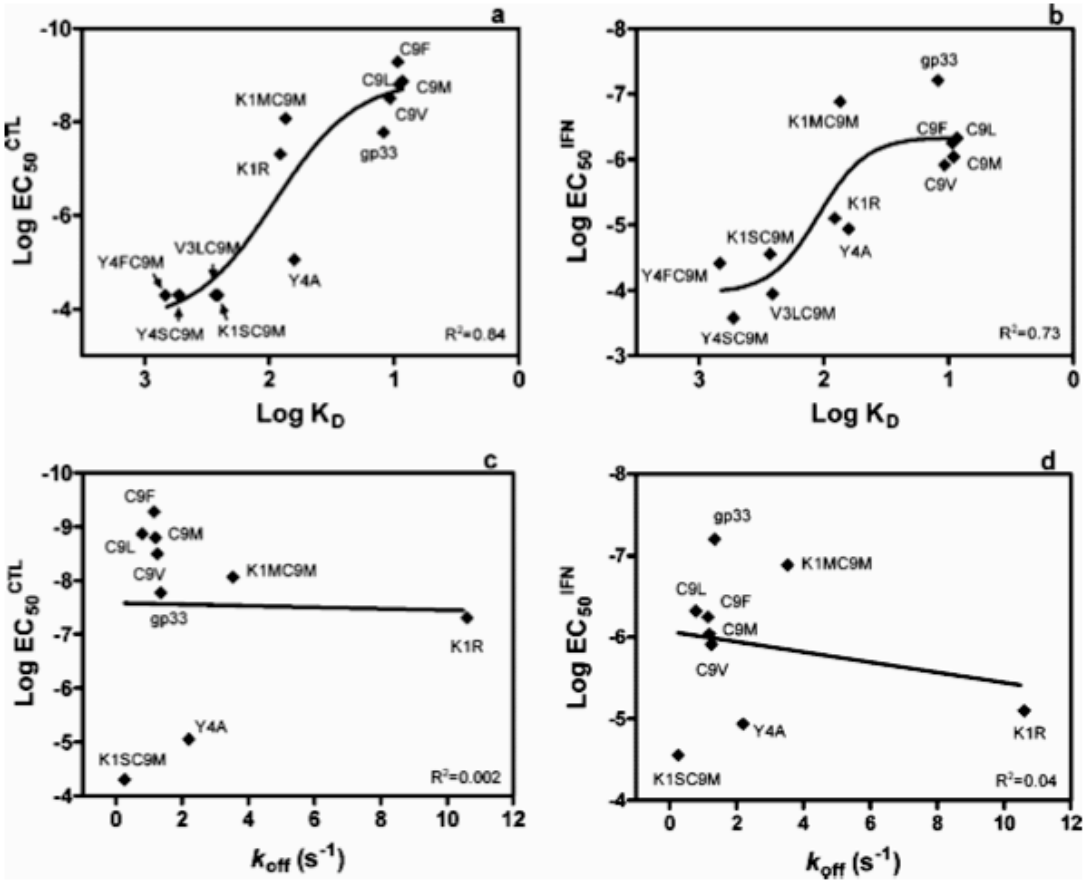


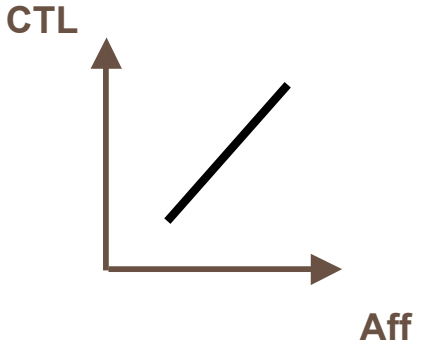


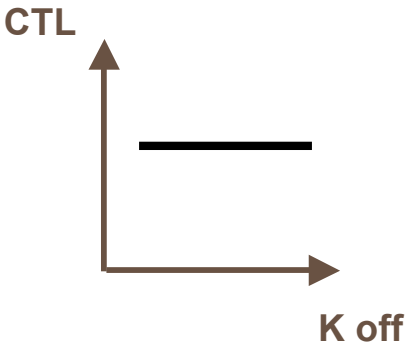


**FIGURE 5.** CTL response and IFN-γ production are correlated with binding affinity of peptide/$D^b$ to P14 TCR. *a* and *b*, Correlations between log $EC_{50}^{CTL}$ and log $K_D$ (*a*), log $EC_{50}^{IFN}$ and log $K_D$ (*b*). All the data points are shown in Table II. The $EC_{50}^{CTL}$ and $EC_{50}^{IFN}$ values are in unit of M, and $K_D$ in μM. The solid lines are the fittings to Boltzmann sigmoidal equation as follows: Y = bottom + (top − bottom)/(1 + exp((V50 − X)/slope)), using GraphPad Prism. The $K_D$ values for V3LC9M, Y4FC9M, and Y4SC9M are adopted from a previous report (42). Note that the $EC_{50}^{CTL}$ values for K1SC9M, V3LC9M, Y4FC9M, and Y4SC9M were shown on the graph as 50 μM, although the actual values could be higher than that, but are out of the measurable range with CTL assay. *c* and *d*, Correlations between log $EC_{50}^{CTL}$ and $k_{off}$ (*c*), log $EC_{50}^{IFN}$ and $k_{off}$ (*d*). The solid lines in *c* and *d* are linear fittings using GraphPad Prism 4.01. All of the data points are shown in Table II. The $EC_{50}^{CTL}$ and $EC_{50}^{IFN}$ values are in unit of M.

# L'affinité ne prédit pas toujours l'activation et la réponse lymphocytaire

- **Activation:**
  - Ont été observées :
    - Une diminution de l'activation liée à une augmentation de l'affinité
    - Une augmentation de l'activation liée à une diminution de l'affinité

- **Spécificité**

The Study of High-Affinity TCRs Reveals Duality in T Cell Recognition of Antigen: Specificity and Degeneracy
*D Donermeyer et al; Journal of Immunology, 2006,*

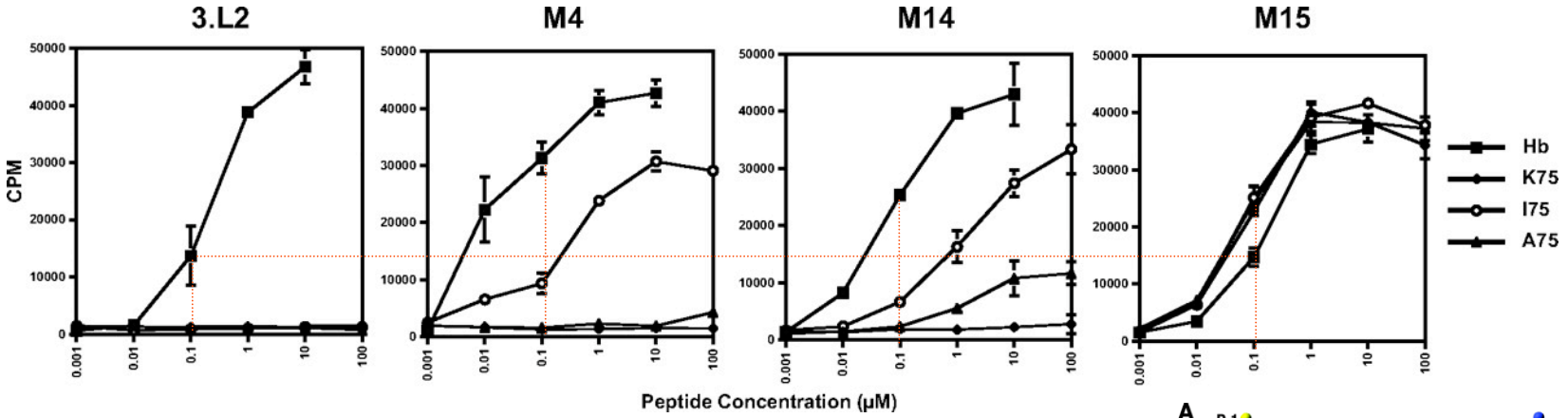


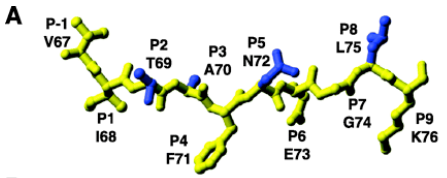


B

| T cell | CDR mutations β:1 2 3 α:1 2 3 | $K_D$ ($k_{off}/k_{on}$) nM | Half-Life s | $k_{on}$ $M^{-1}s^{-1}$ | $k_{off}$ $s^{-1}$ |
|---|---|---|---|---|---|
| M1 | ○○○ ○○○ | 19,860 ± 3,630 | 6.8 ± 0.7 | 5,220 ± 410 | 0.1023 ± 0.0107 |
| M4 | ○○○ ○○● | 580 ± 185 | 28.5 ± 0.8 | 42,670 ± 17,430 | 0.0243 ± 0.0007 |
| M14 | ○○● ○○● | 81 ± 2 | 48.9 ± 2.4 | 173,500 ± 3,500 | 0.0141 ± 0.0007 |
| M15 | ○○● ●○● | 25 ± 5 | 104.4 ± 9.1 | 281,500 ± 34,800 | 0.0068 ± 0.0006 |

**Degeneracy in the recognition of Hb correlates with increased affinity**. CD4+ T cell hybridomas expressing 3.L2, M4, M14, and M15 TCRs were stimulated with the indicated peptide concentrations of Hb or APLs of Hb at the P8 (75) position using CH27 as APC. The APLs are designated as described in Fig. 2. The level of T cell stimulation was determined using a bioassay for IL-2. The cpm values of [3H]TdR incorporation into CTLL-2 cells represent the mean ± SD of triplicate values of a representative experiment (n > 3).

UPMC PARIS UNIVERSITAS

B. Bellier

# Activation T : un système dynamique

# Stimulation réitérative du lymphocyte: « kinetic proofreading » model

- **Activation du lymphocyte T** si **interaction TCR/CMH-Ag suffisante (seuil d'activation)**

- **Interactions :**
  - Force d'interaction (Affinité)
  - Temps d'interaction (Koff)
  - Nombre d'interactions (x n; Avidité)

- **Activation progressive des molécules de signalisation (phosphorylation) : seuil d'activation**

- **Seuil critique pour initier une activation fonctionnelle**

- **Si interaction insuffisante, (dissociation du complexe TCR/CMH-Ag) avant initiation de l'activation: les groupements phosphates seront éliminés par les phosphatases cellulaires** (McKeithan 1995)

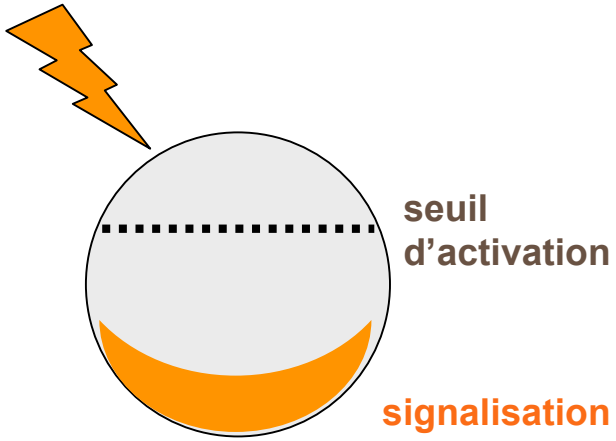


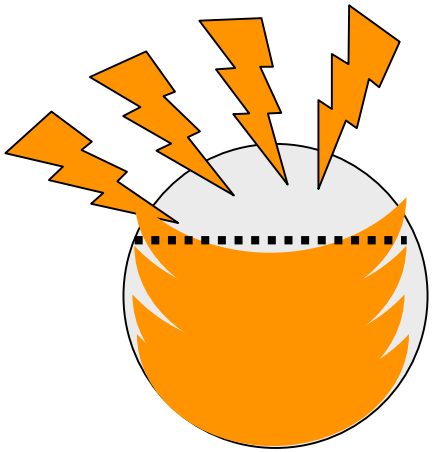

# Variabilité du niveau du seuil d'activation: T naïf vs T mémoire

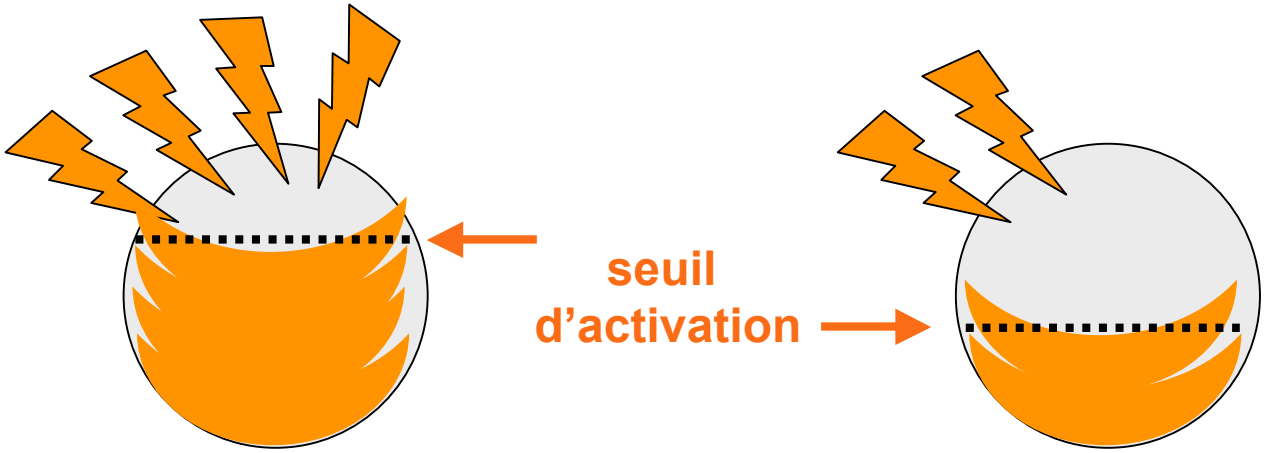


T naïf

T mémoire

# Seuil d'activation: T naïf vs T mémoire

## Spleen cells+Ag

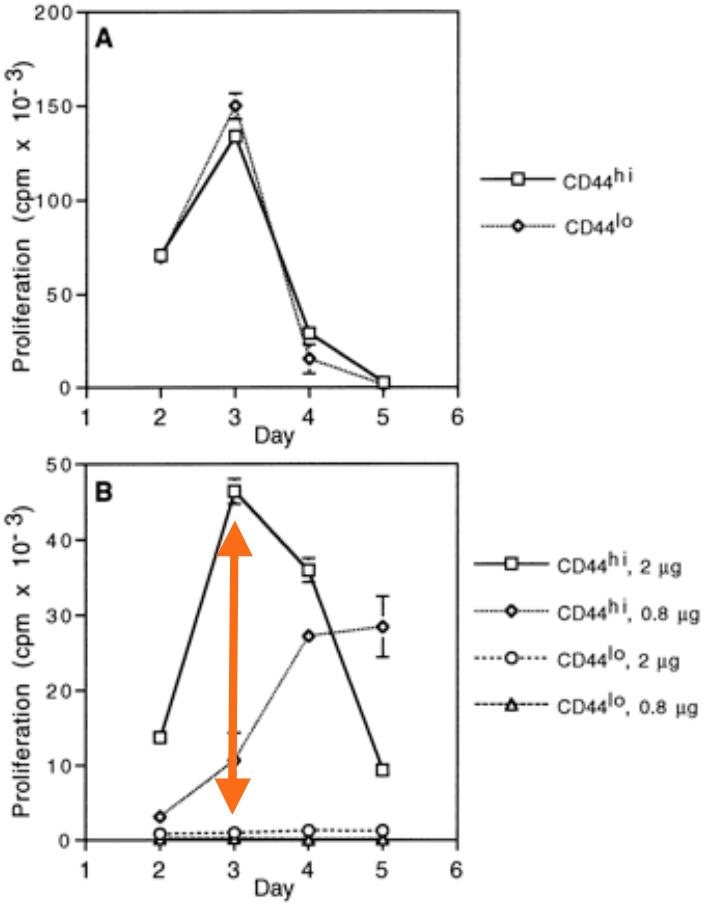


## Beads H-2Kb+Ag

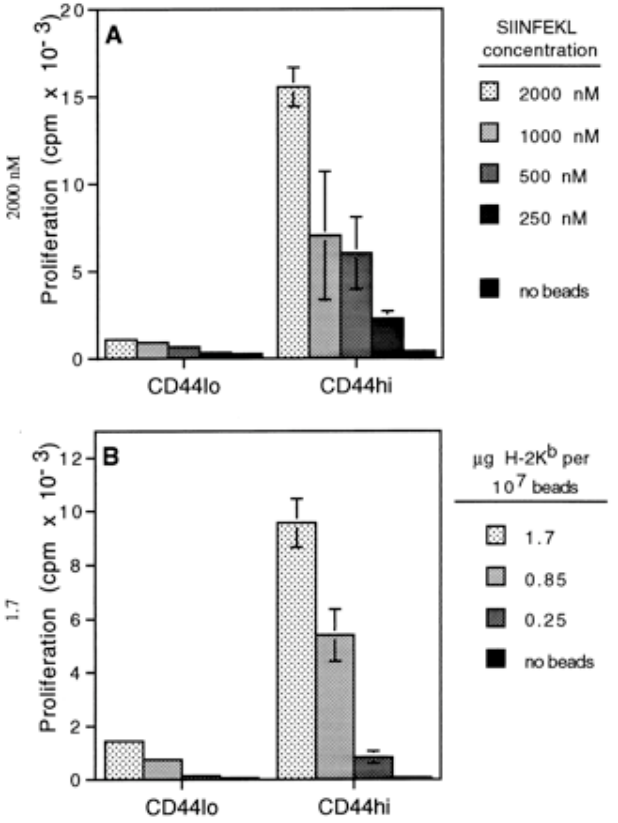


## Beads H-2Kb+Ag

*Curtsinger, JI 1998*

- **Proliferation of OT-1 CD8⁺ LNC in response to Kb/OVA$_{257–264}$ and rIL-2 is predominantly due to the CD44$^{high}$ subset of cells. *A*, LNC (5 x 10$^4$-sorted CD44$^{low}$CD8⁺ and CD44$^{high}$CD8⁺) from OT-1 mice were cultured with 1 x 10$^5$ latex beads coated with H-2K$^b$ at 1.7 *µ*g protein/10$^7$ beads and pulsed with OVA$_{257–264}$ peptide at the indicated concentration.**

B. Bellier

# Dynamique de l'interaction
# Affinité versus Avidité

**force du signal**

Affinité

Avidité

++++

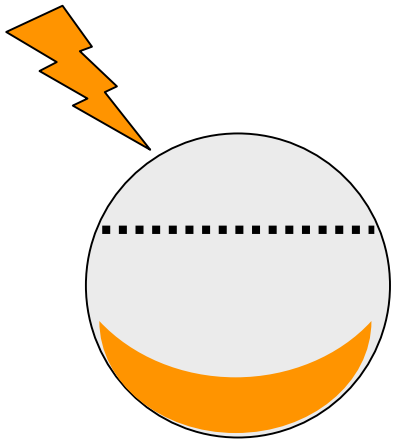

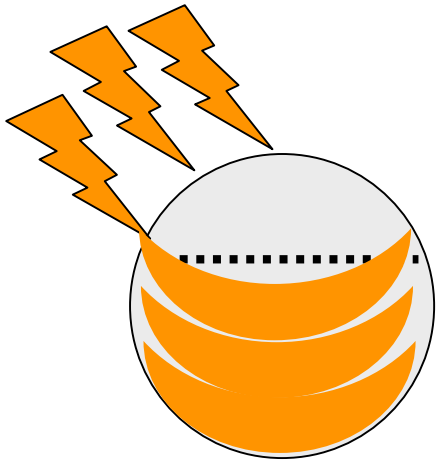

x n

**sommation du signal**

+

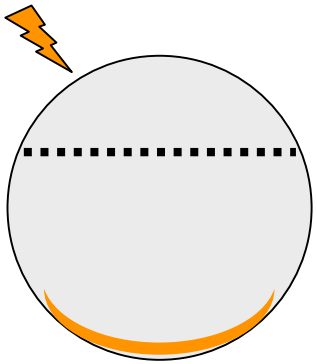

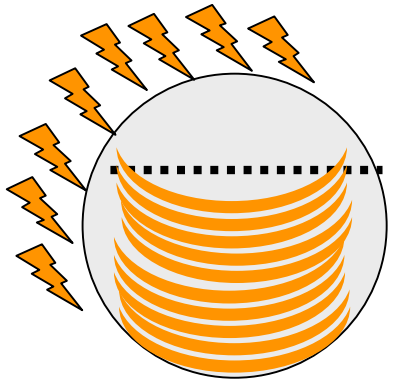

x n

# Relevance physiologique
# DC scanning

- Contacts multiples avec complexes CMH-Ag à la surface des DC

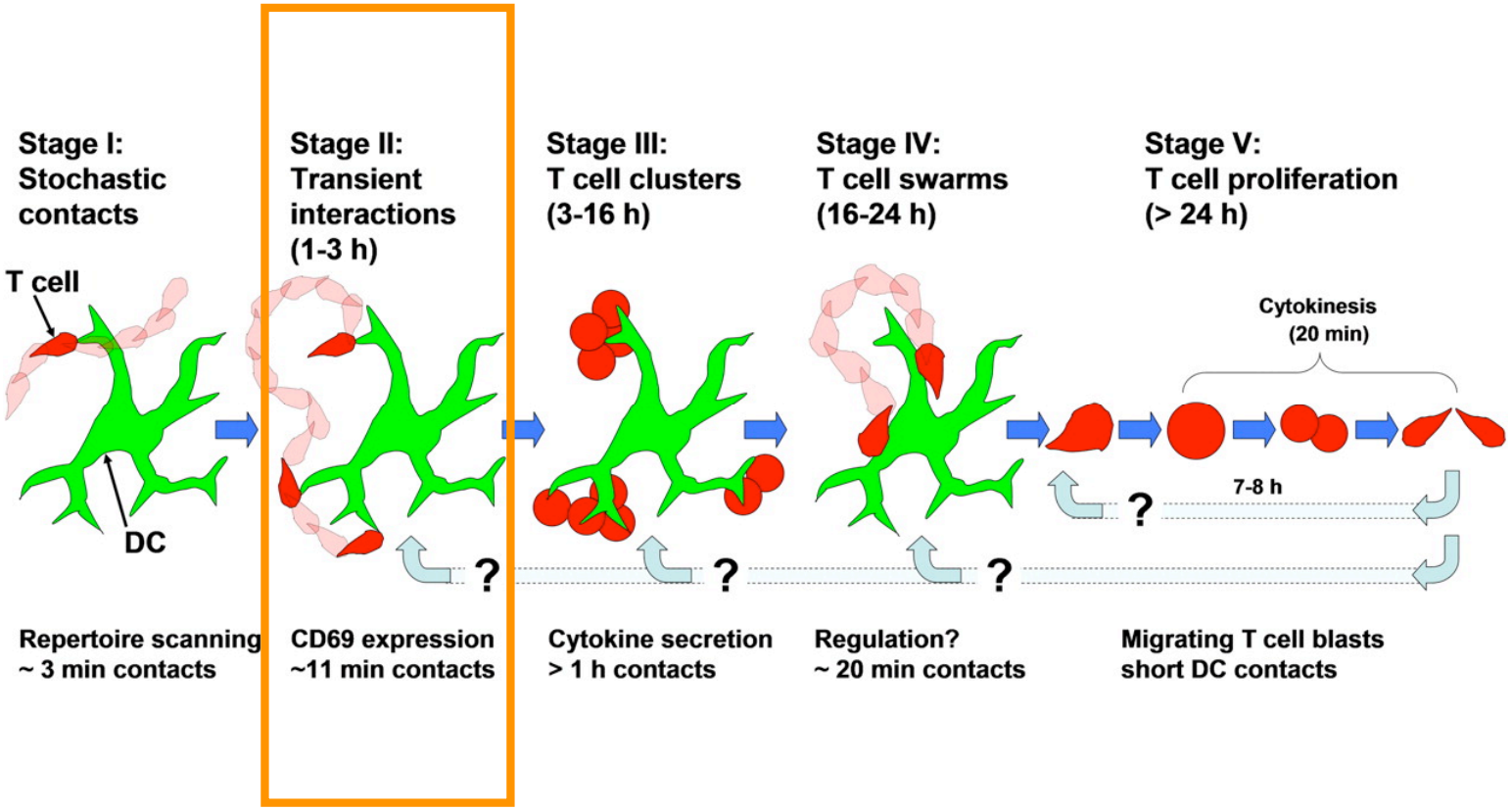

# Nombre d'interactions TCR/CMH-Ag dépend de l'affinité du TCR

Immunity, Vol. 5, 137–146, August, 1996, Copyright ©1996 by Cell Press

## Correlation Between the Number of T Cell Receptors Required for T Cell Activation and TCR–Ligand Affinity

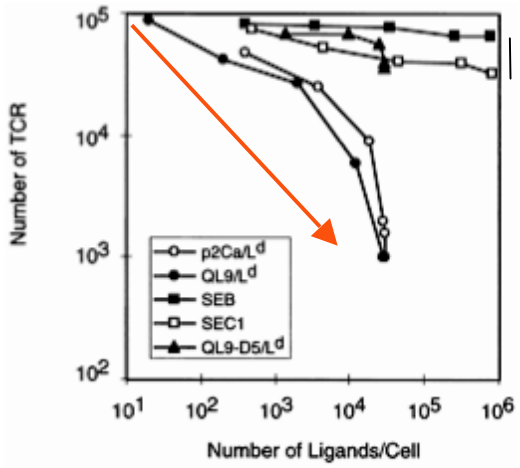


Figure 4. Relationship of Number of Ligands per Target Cell and the Number of TCRs Required for Activity

The number of 2C TCR required for recognition of various ligands was plotted as a function of the number of ligands on the target cell. The number of p2Ca–L$^d$, QL9–L$^d$, QL9-D5–L$^d$, SEB–class II, or SEC1–class II complexes was calculated from the $K_a$ of the peptide or SE for MHC and the concentration of peptide or SE added in the assay. The number of TCR required for recognition was determined from the concentration of 1B2 Fab fragments required at 50% inhibition of cytolysis, using a $K_a$ of $2 \times 10^9$ M$^{-1}$ and 100,000 TCRs per T cell, as described in Experimental Procedures. Data are taken from Table 2.

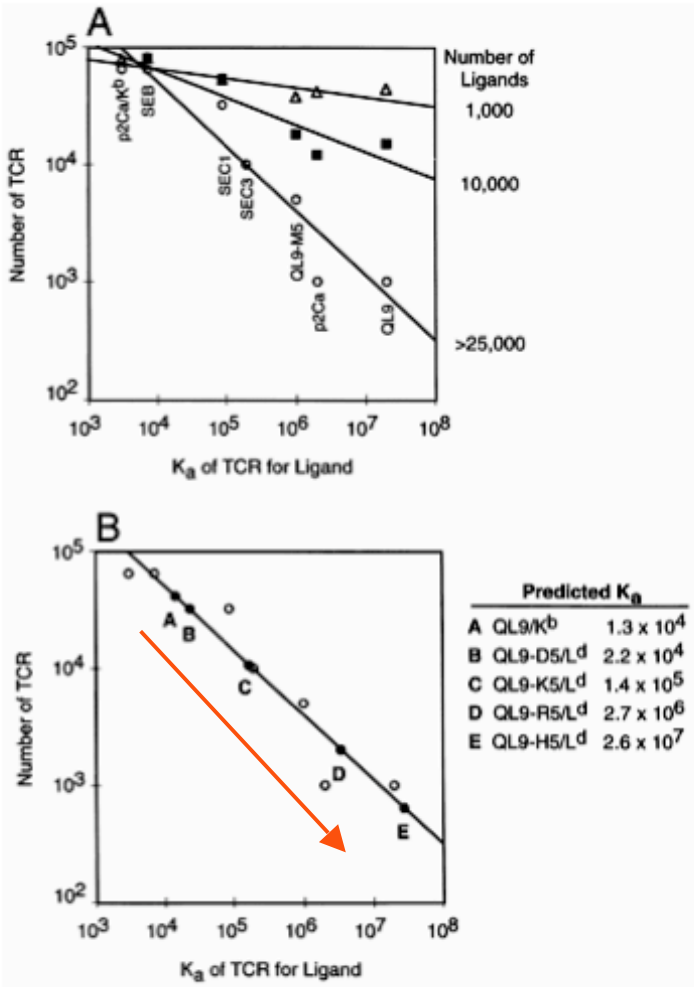


Figure 5. Correlation Between the Binding Affinity of the TCR for Its Ligand and the Number of TCRs Required for T Cell Activity

(A) $K_a$ values from previous reports are summarized in Table 1. The number of TCR at >25,000 ligands (open circles) was determined at saturating ligand concentrations for each of the peptides or superantigens that have a published binding affinity for the 2C TCR. The number of TCRs at 1,000 (open triangles) and 10,000 (closed squares) ligands were calculated by regression analysis from the data summarized in Table 2.

(B) $K_a$ values for the TCR interaction with the indicated peptide–class I complexes were predicted from the number of TCRs required for activity. The curve determined from known $K_a$ values for several TCR–ligand interactions was plotted versus number of TCRs at saturating ligand concentrations (open circles) to generate a standard curve. The inhibition analysis was used to determine the number of TCRs required at $3 \times 10^{-5}$ M QL9-H5, QL9-R5, QL9-H5 and $10^{-4}$ M QL9-D5 with T2-L$^d$ and $10^{-4}$ M QL9 with T2-K$^b$. These values were plotted on the standard curve (closed circles) to calculate by linear regression a predicted $K_a$ value for TCR binding to each of the peptide–class I complexes.

Modèle:

Clone 2C anti-AlloAg

Spé p2Ca/Ld; QL9/Ld

Nb ligands: Δ[peptide]

Nb TCR: [Fab 1B2], bloque TCR

Affinité: Mutants de QL9

# Nombre d'interactions TCR/CMH-Ag: aspects moéculaires

- **1 à 50 complexes CMH-Ag sur APC pour activer LyT**
- **Engagement multiple des TCR pour un complexe CMH-Ag**
  - N= 200 contacts répétitifs (Valitutti 1995)
- **Temps de contact cellulaire requis ? (Long / Court)**
- **Temps de contact TCR/CMH-Ag limité pour assurer des engagements répétés des TCR**
- **Engagement répété de la même molécule de TCR  vs différentes molécules de TCR ?**

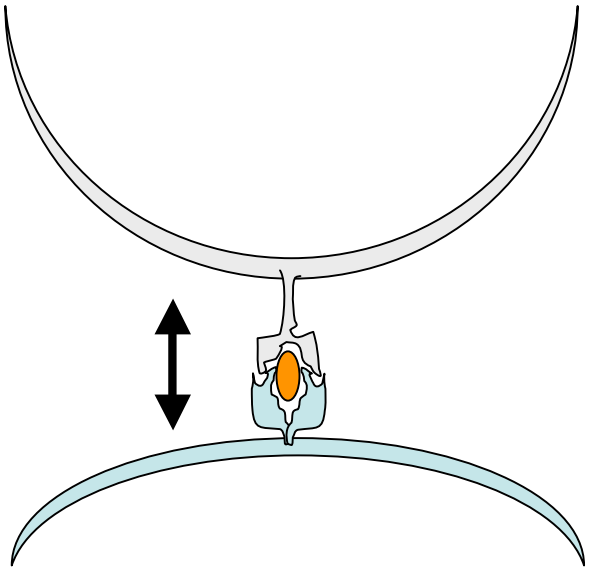

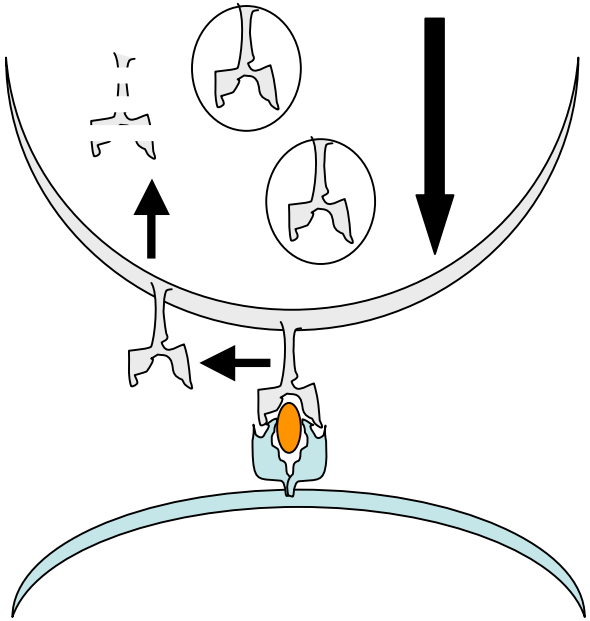

**Serial triggering of many T-cell receptors by a few peptide-MHC complexes**
**Valitutti, Nature 1995**

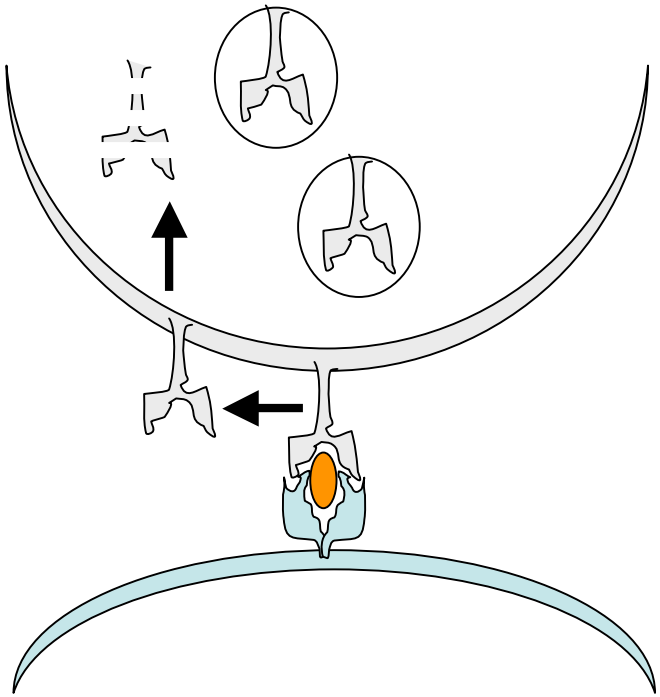

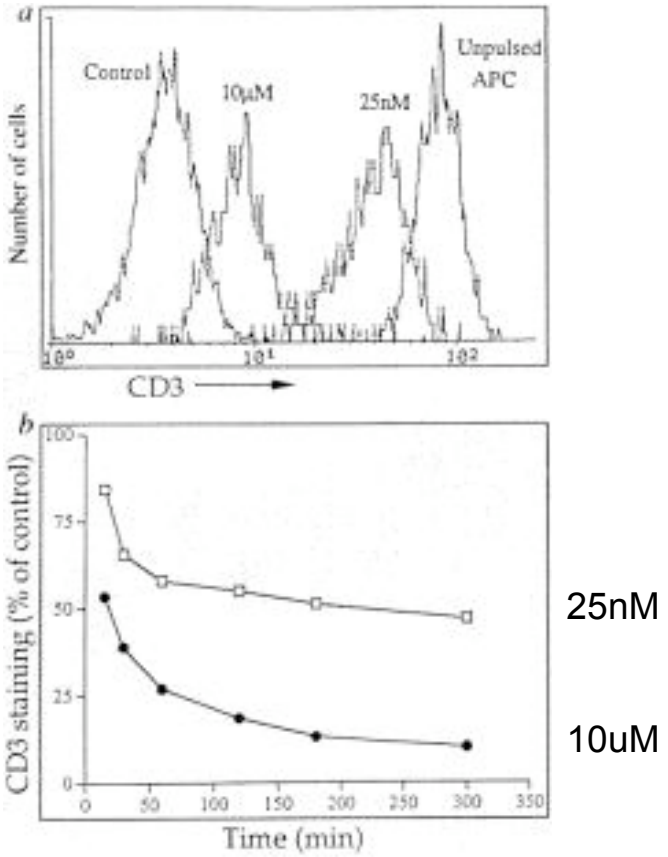


**>> internalisation des complexes moléculaires « TCR »**

T cells conjugated with peptide-pulsed APCs undergo an antigen-dependent **downregulation of the TCR**/CD3 complex.

# Nombre d'engagements

## *Serial triggering of many T-cell receptors by a few peptide-MHC complexes Valitutti, Nature 1995*

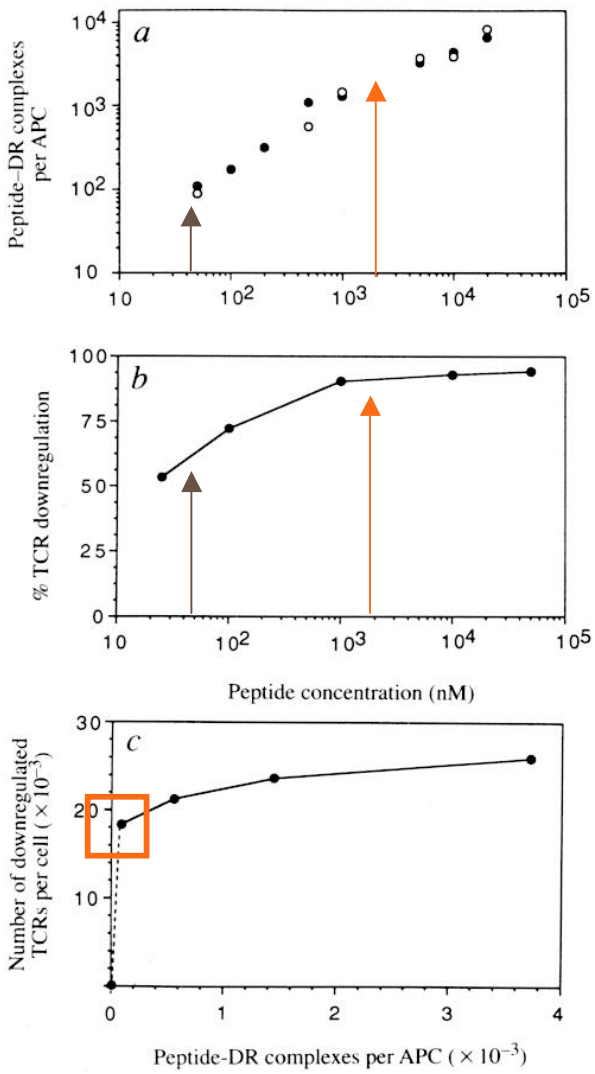


we measured at different antigen concentrations the number of complexes per APC and the number of TCRs downregulated after T-APC interaction. In one series of experiments, EBV-B cells were pulsed with different concentrations of **125 I-labelled peptide** and the number of peptide-DR complexes per cell was calculated at each peptide concentration Figure 3(a). In parallel experiments, the fraction of TCRs downregulated by APCs pulsed in the same conditions was measured Figure 3(b). From comparison of the two curves it is estimated that **APCs pulsed with high peptide concentrations (20 micromolar) display approximately 7,500 complexes and induce downregulation of 93 percent of TCRs.** Strikingly, **APCs pulsed with a low peptide concentration (50 nM) display only approximately 100 peptide-DR complexes, yet they downregulate 62 percent of TCRs.** The relationship between the number of peptide-DR complexes per APC and the number of TCRs downregulated per T cell is shown in Figure 3(c). This plot clearly shows that each peptide-DR complex must engage a large number of TCRs in successive rounds. This effect is dramatic at low complex density, where approximately **100 complexes can trigger up to 18,000 TCRs**, but is less marked at high complex density, indicating that **a single peptide-DR must be able to trigger 180 TCRs in successive rounds.** This figure may increase at lower complex density and could be an underestimate as it is unlikely that all complexes present on an APC may be available to the responding T cell.

B. Bellier

# Internalisation du TCR

## Coombs et al 2002

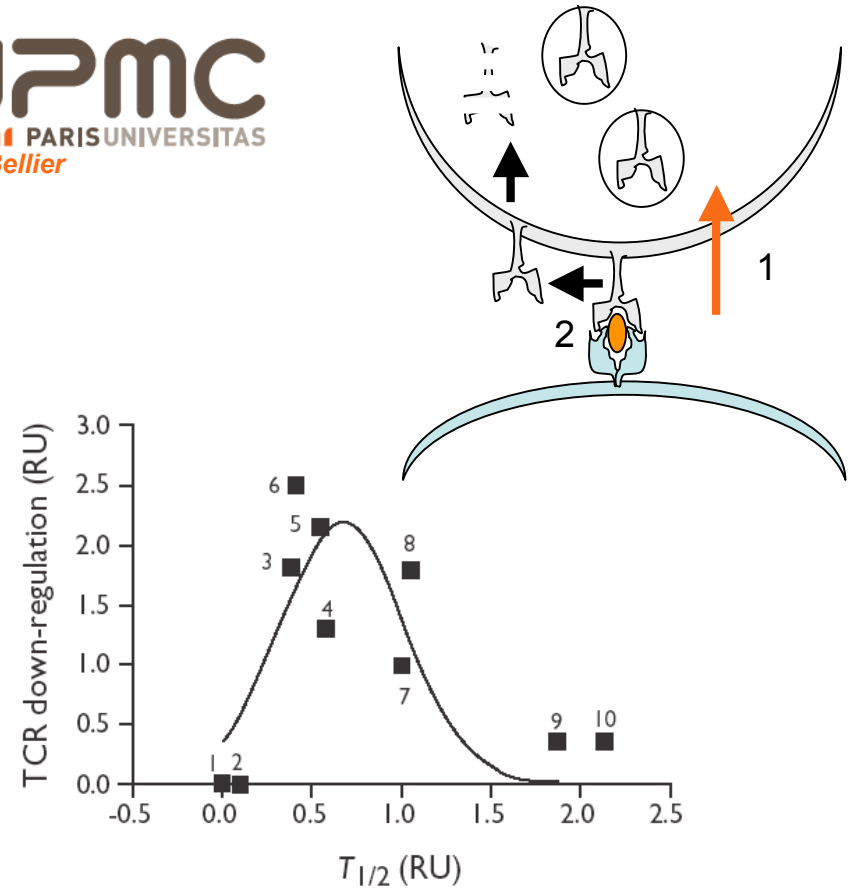


**TCR down-regulation as a function of TCR-pMHC half-life.**
Data are derived from 5-h TCR down-regulation experiments done with a panel of TCR mutants derived from a Kb-VSV-specific TCR (N30.7). Each point represents the indicated TCR-pMHC pair: 1, V98D- Kb-VSV; 2, V98L-Kb-VSV; 3, N30.7-KbA158T-VSV; 4, G99A-KbA158T-VSV; 5, G97/99A-KbA158T-VSV; 6, G97A-KbA158T-VSV; 7, N30.7- Kb-VSV; 8, G97A-Kb-VSV; 9, G97/99A- Kb-VSV; 10, G99A-Kb-VSV. Half-lives are shown as relative units (RU) normalized to the half-life for the N30.7-Kb-VSV (number 7) interaction4. TCR down-regulation data are shown as RU normalized to TCR down-regulation measured for N30.7 hybridomas that were interacting with 10-4 - 10-5 M VSV peptide.

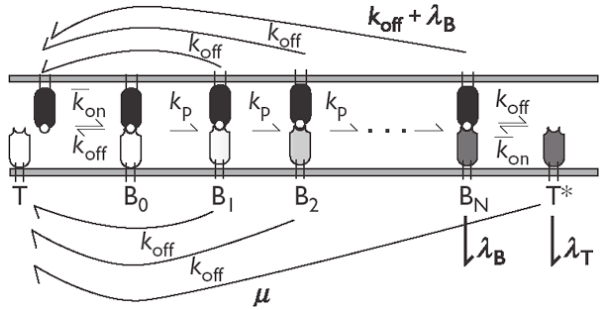


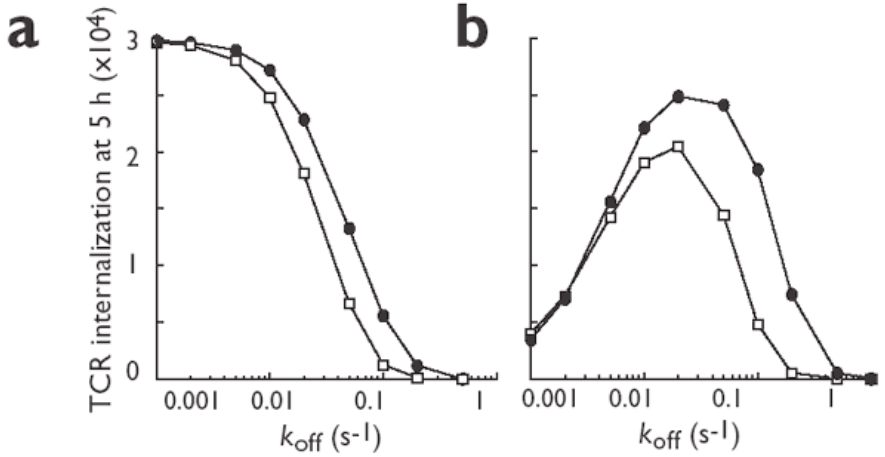


TCR internalization as a function of the dissociation rate constant. Results are shown for the monomer model (closed circles) and the dimer model (open squares). (a) Only activated bound TCRs are internalized, lambdaB = lambdaD = 0.003 s-1, lambdaT = 0 s-1. (b) **Only unbound activated TCRs are internalized**, lambdaB = 0 s-1, lambdaT = 0.003 s-1.

**> Internalisation du TCR dépend:**

- –De la constante de dissociation
- –De temps de contact

**> Après libération du CMH-Ag = Modèle 2**

# Interactions en série

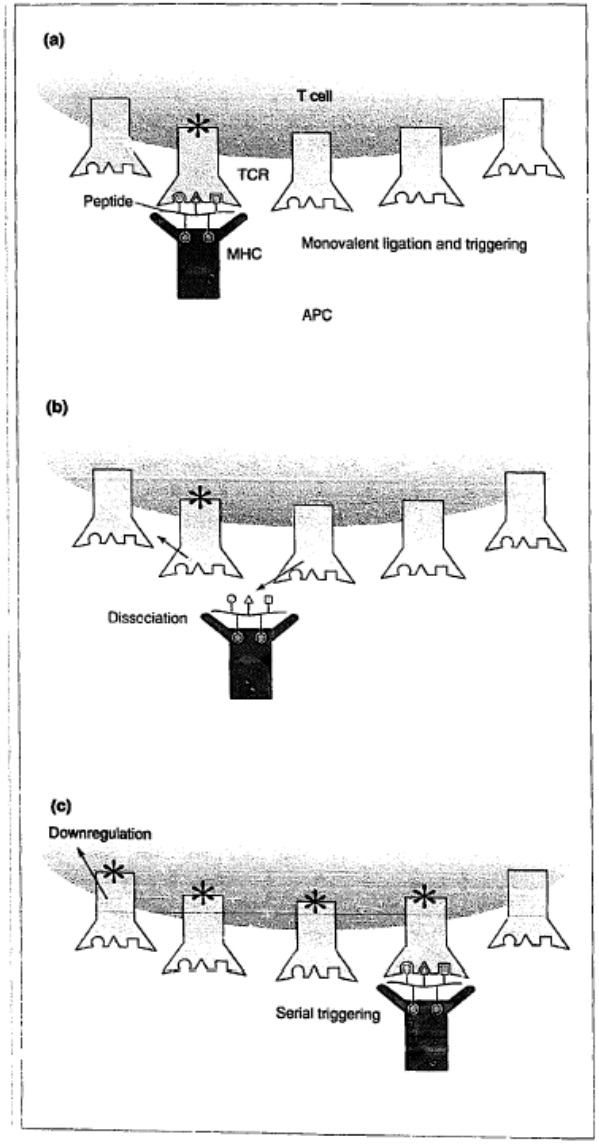


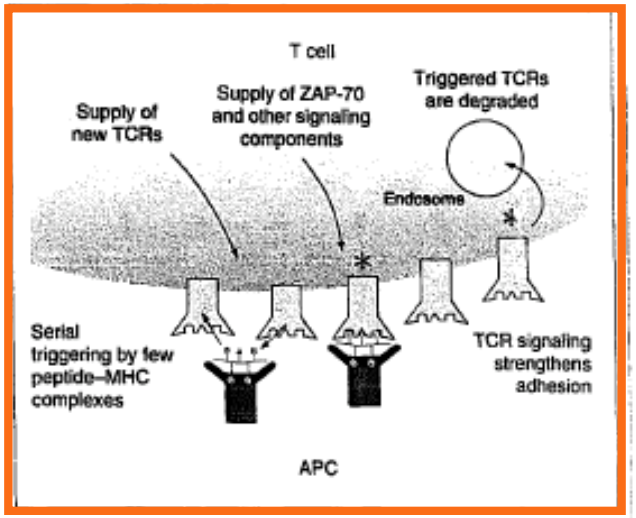


**Fig. 3.** *Parameters that influence TCR triggering and signaling at the level of the T-cell–APC interaction. Sustaining the process requires a continuous supply of signal transduction components from the cytosol, as well as new TCRs to substitute for those that are downregulated and degraded*[39]*. Cell–cell adhesion is boosted by TCR signaling and favors TCR engagements with peptide–MHC complexes. Abbreviations: see Fig. 1 legend.*

Serial triggering of TCRs: a basis for the sensitivity and specificity of antigen recognition

**Salvatore Valitutti and Antonio Lanzavecchia**

UPMC PARIS UNIVERSITAS

B. Bellier

# Serial triggering of TCRs: a basis for the sensitivity and specificity of antigen recognition

Salvatore Valitutti and Antonio Lanzavecchia

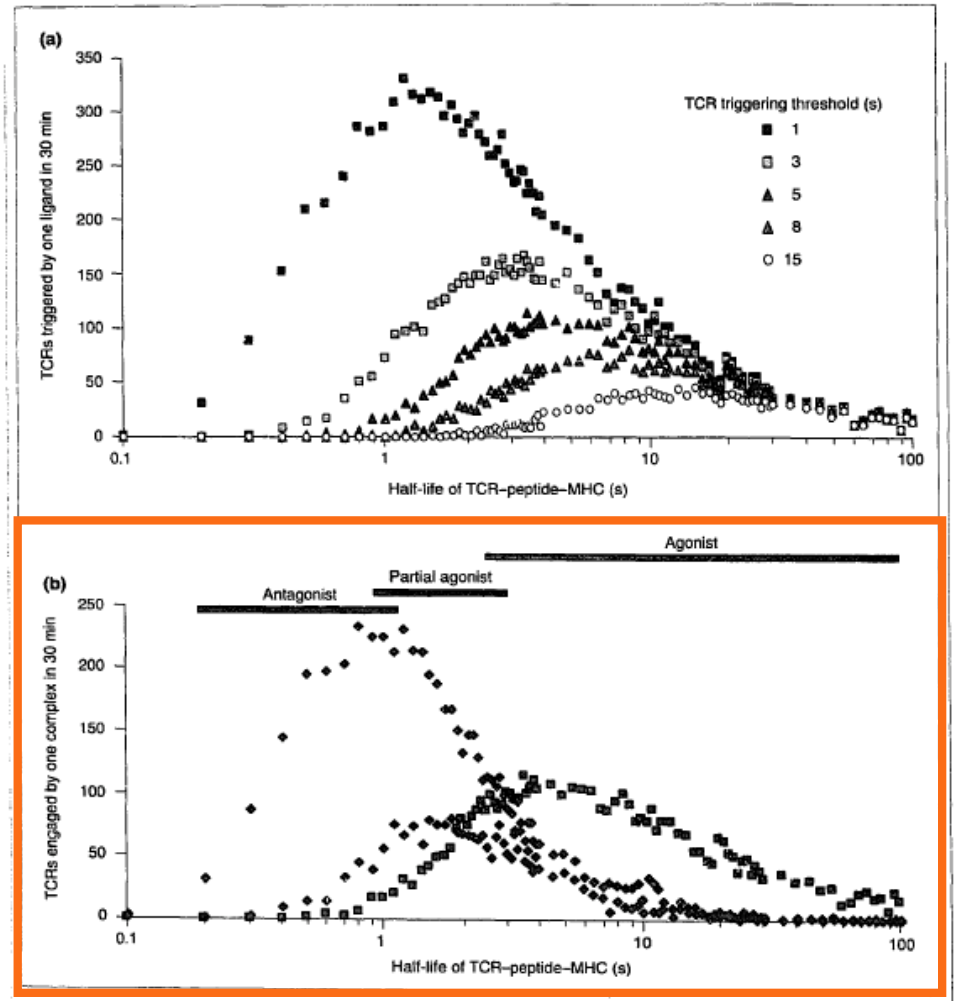


**Fig. 2.** *Serial TCR triggering or inactivation as a function of complex stability and time required for TCR triggering. (a) Simulation describing the number of TCRs triggered in 30 min as a function of the half-life of TCR–peptide–MHC interactions. Each curve is calculated for times required for TCR triggering ranging 1–15 s. (b) Simulation describing the number of TCRs fully triggered (green), partially triggered (blue) or inactivated (red) as a function of the half-life of TCR–peptide–MHC interaction. It is assumed that ligation for >5 s results in full TCR triggering, ligation for 3–5 s in partial triggering and ligation for 1–3 s in TCR inactivation. Abbreviations: see Fig. 1 legend.*

| | Agonist | Antagonist |
|---|---|---|
| T1/2 | 3-10 | 0.5-1 |
| #TCR | 100 | 250 |

# Paramètres d'activation

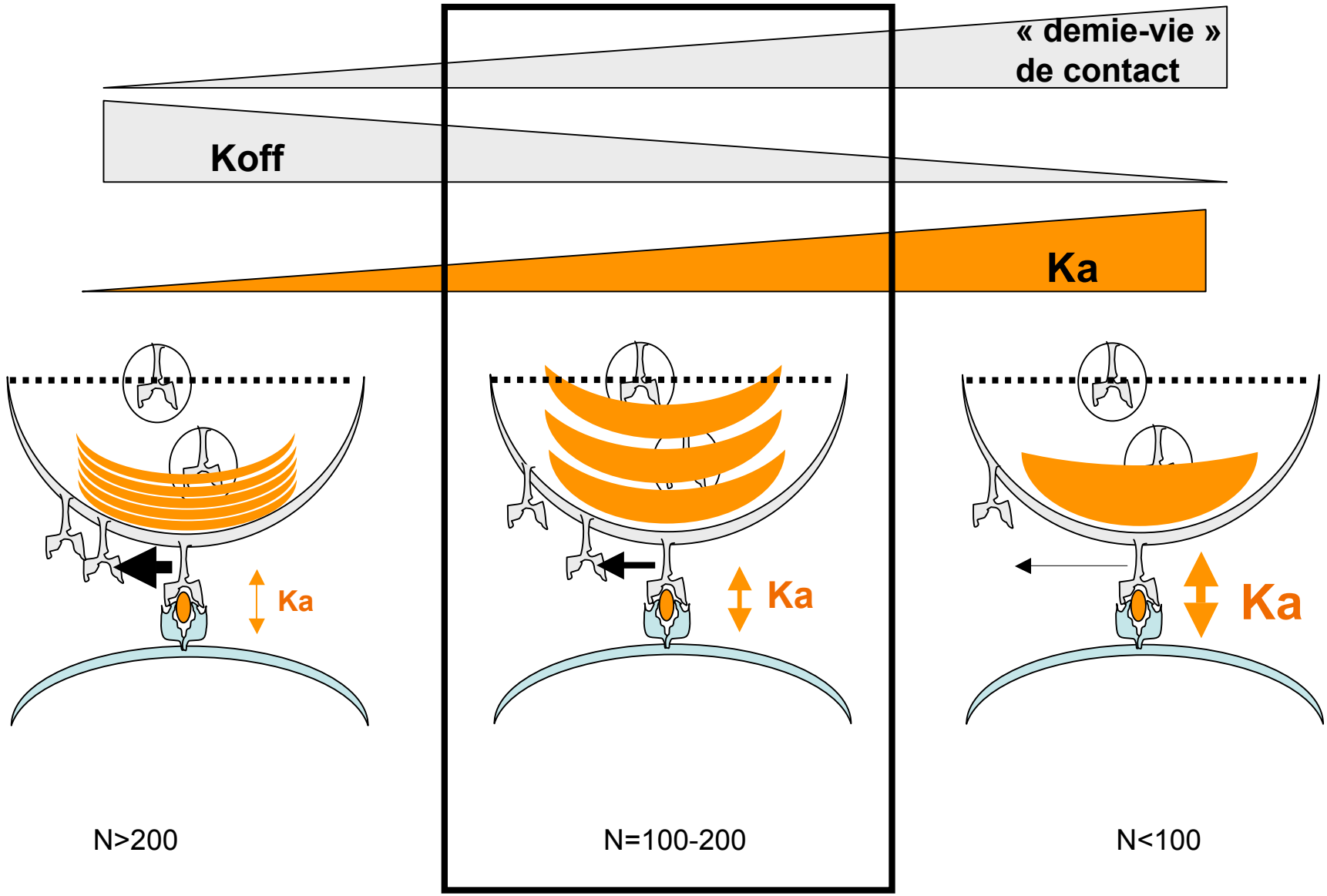

# Importance de la « demie-vie » de contact

L.J. Carreño et al. / Immunobiology 211 (2006) 47–64

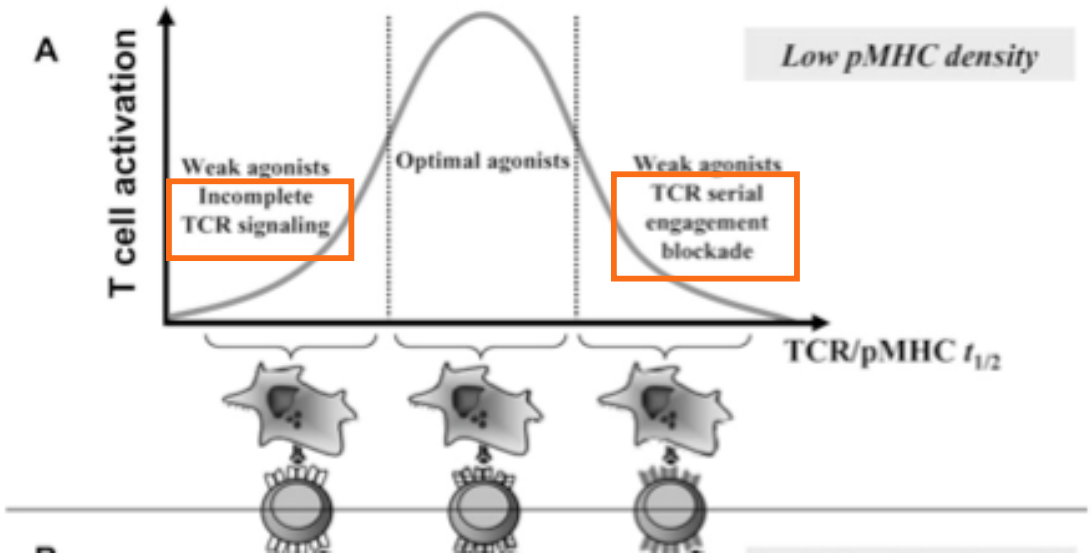


**Fig. 2.** T cell activation depends on TCR/pMHC interaction half-life and pMHC density. (A) When T cells interact with cognate pMHC at low density on the APC, efficient activation takes place within an optimal range of TCR/pMHC interaction half-life. Interactions with short half-lives cannot complete necessary intracellular signals for T cell activation, due to impairment on TCR kinetic proofreading. TCR/pMHC interactions with excessively long half-lives impair T cell activation due to TCR serial engagement blockade. At low pMHC density, the plot of T cell activation versus TCR/pMHC half-life results in a Gaussian distribution, in which only pMHCs that interact with intermediate half-lives with the TCR behave as agonists (Kalergis et al., 2001; Coombs et al., 2002). (B) When T cells interact with cognate pMHC at high density on the APC, T cell activation can take place when the half-life of the TCR/pMHC interaction is intermediate or high, because serial engagement requirement no longer applies (Gonzalez et al., 2005). At high pMHC density, the plot of T cell activation versus TCR/pMHC half-life results in a sigmoid distribution, in which pMHCs that interact with intermediate and long half-lives with the TCR behave as agonists.

B. Bellier

# Importance de la synapse immunologique pour favoriser la multiplication des contacts

- **Favorise interactions multiples TCR/CMH-Ag**
- **Rôle dans la transduction du signal ?**
  - Formation de la synapse est associée à l'activité PI3K
  - Blocage de la synapse empêche signal calcique (tardif) et la production de cytokine (IFNg) mais ne perturbe pas les événements de signalisation précoces (phosphorylation ERK)
- **Lien étroit entre activation T et maintien de la structure « synapse »**
  - De la meme façon qu'il existe des paramètres d'interaction du TCR optimum, la formation des suprastructures cSMAC/pSMAC dépend de la demi-vie d'intéraction du TCR

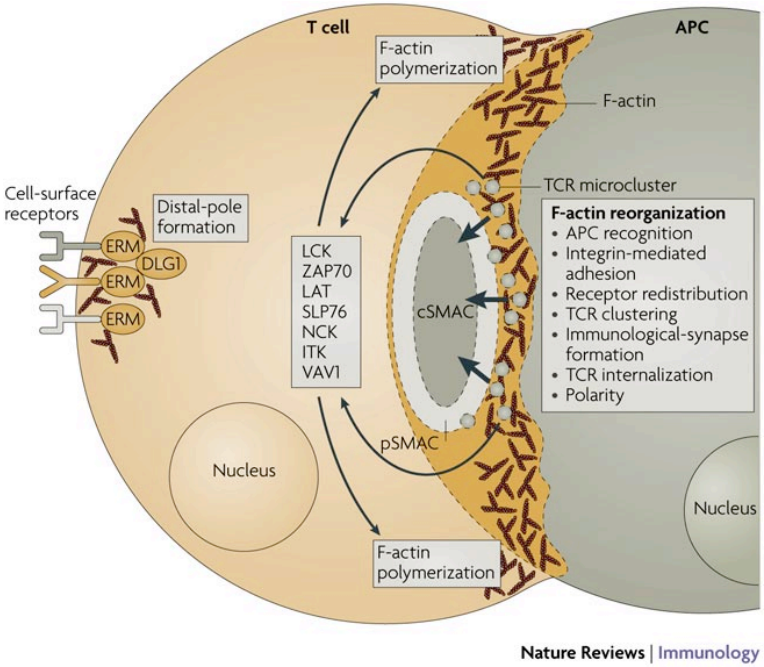


Recruitment and activation of proximal signalling intermediates — such as lymphocyte-specific protein tyrosine kinase (LCK), ZAP70 (-chain-associated protein of 70 kDa), LAT (linker for activation of T cells), SLP76 (SRC homology-2-domain-containing leukocyte protein of 76 kDa), NCK (non-catalytic region of tyrosine kinase), ITK (interleukin-2-inducible T-cell kinase) and VAV1—is probably initiated at sites of T-cell receptor (TCR)-microcluster formation[80, 84]. Recruitment of these molecules leads to the activation of filamentous (F)-actin-regulatory proteins, which control actin polarization in T cells. Interestingly, signals that arise from TCR microclusters not only induce F-actin polymerization, but are required for the stable formation and movement of TCR microclusters, and ultimately lead to the organization of the mature immunological synapse (consisting of the central and peripheral supramolecular activating clusters; cSMAC and pSMAC, respectively)[13, 22, 29, 80]. In addition, global F-actin reorganization resulting from T-cell activation leads to lamellipodium formation and distal-pole formation, facilitating T-cell–APC (antigen-presenting cell) recognition[11]. DLG1 (discs-large homologue-1)[61], ERM (ezrin, radixin and moesin) and F-actin also polarize to the rear of the T cell to form the distal-pole complex[11, 48]. It is thought that this complex recruits some receptors to the rear of the cell, away from the immunological synapse.

# Conséquences sur l'immunodominance



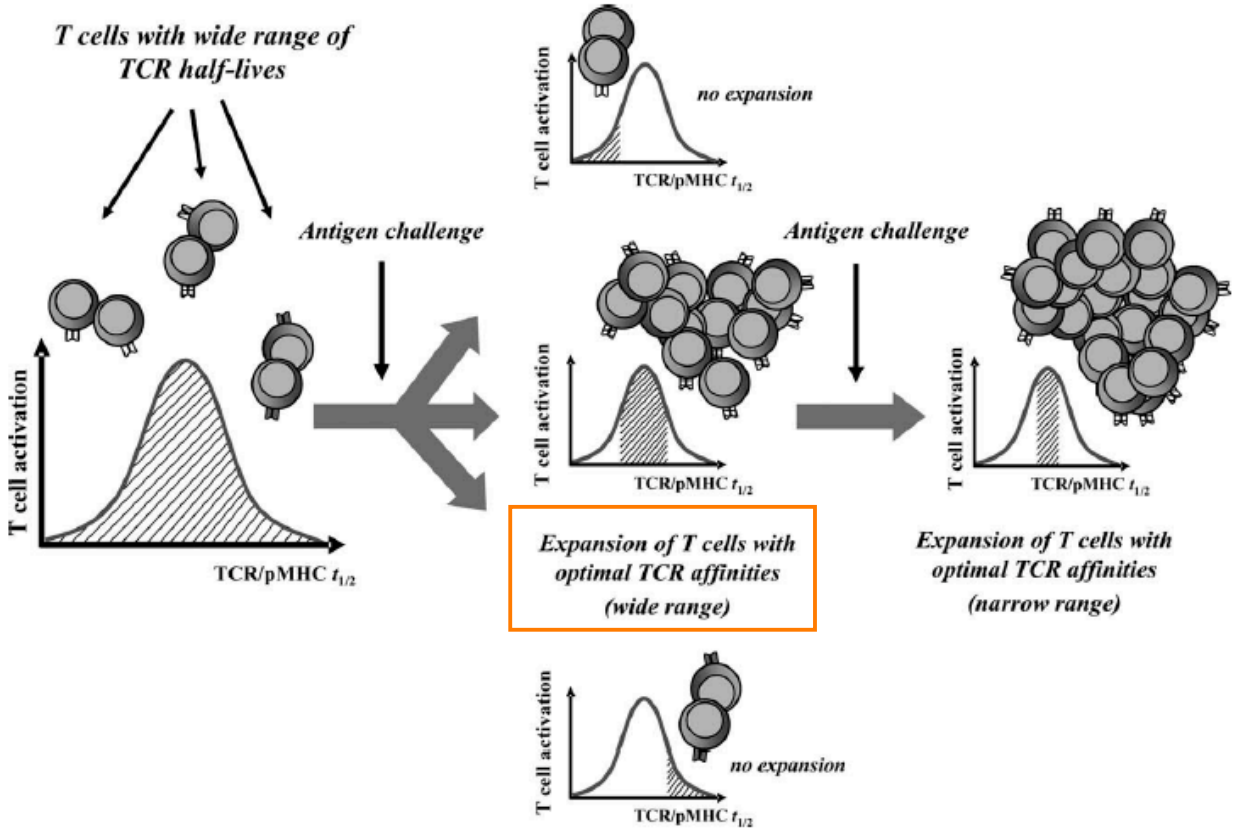


Fig. 3. Clonal expansion of T cells in response to antigenic challenge is determined by the half-life of TCR/pMHC interaction. Before antigen challenge, the T cell population shows a wide range of half-lives for the TCR/pMHC interaction. After the first antigen challenge, only T cells bearing TCRs with optimal half-lives are clonally expanded and the global TCR/pMHC half-life of the responding T cells shifts towards an optimal value. Although subsequent antigenic challenges do not lead to a significant increase in the overall TCR affinity of the T cell population, there is a selection of T cells within a narrower range of TCR/pMHC half-lives.

# Influence de la densité de complexe CMH-Ag

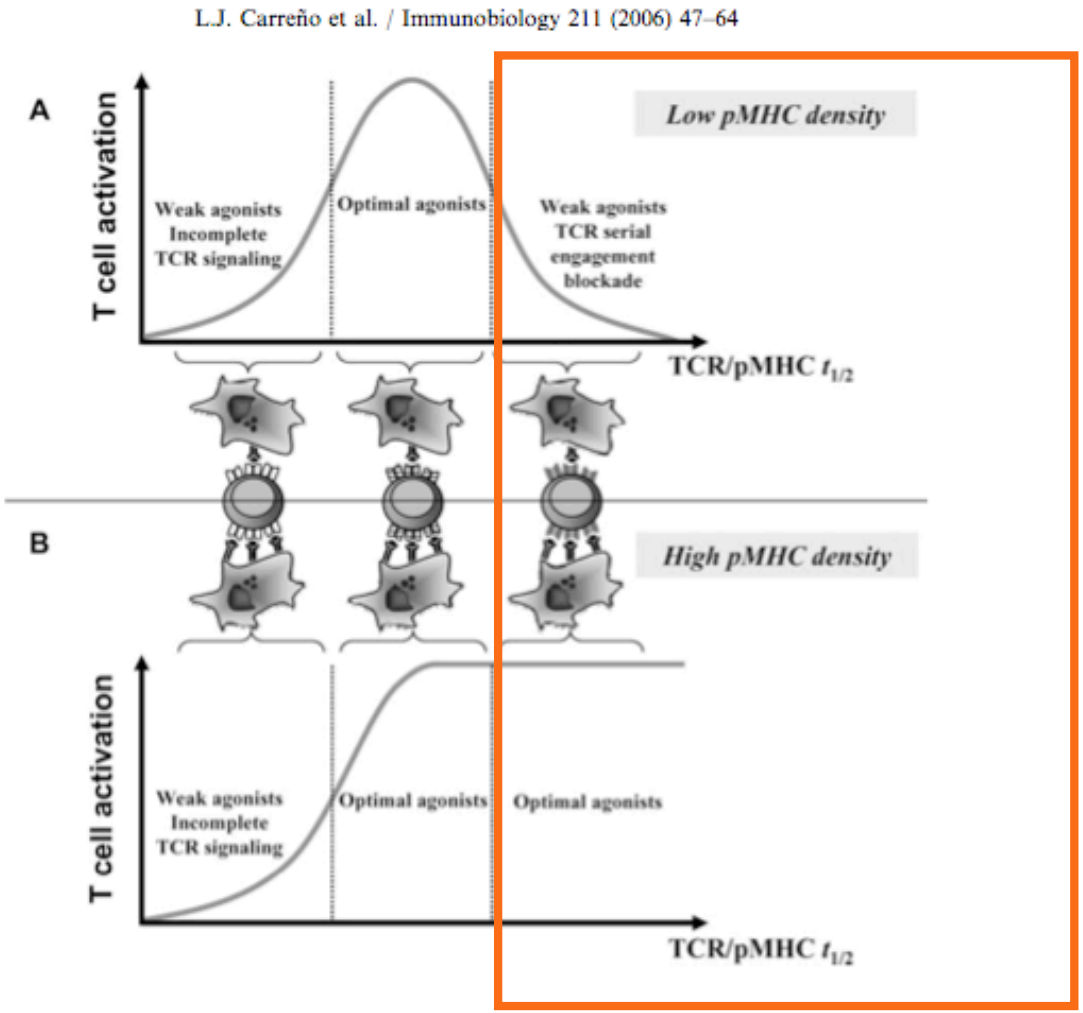

UPMC PARIS UNIVERSITAS

B. Bellier

# la diminution d'expression des CMH limite la réactivité des T

## Cas de l'échappement viral et tumoral:

**A review of viral strategies to evade selected components of the host immune system,** Bruce Wobeser

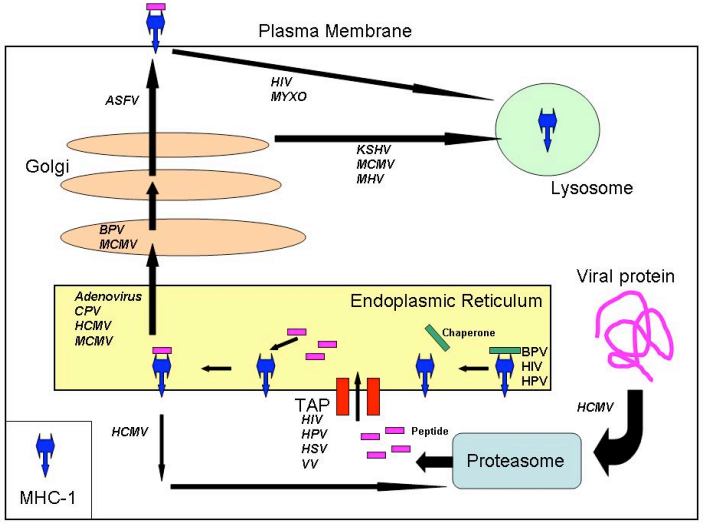


| Virus | Gene / Gene Products | Function |
|---|---|---|
| Adenovirus | E3/19K | Retention of MHC-1 in ER |
| African Swine Fever Virus | Unknown | Dispersion of trans-Golgi network, slowing of MHC-1 to plasma membrane |
| Bovine Papillomavirus | E5 | Retention of MHC-1 in Golgi, repression of MHC-1 gene promoter |
| Cowpox Virus | Unknown early gene | Retention of MHC-1 in ER |
| Human Cytomegalovirus | pp65 | HLA-DR segregation and destruction, phosphorylation of 72-kDa transcription factor |
| | US2 | Destruction of MHC-1 heavy chains |
| | US3 | Retention of MHC-1 in ER |
| | US6 | Inhibition of TAP |
| | US11 | Destruction of MHC-1 heavy chains |
| Human Immunodeficiency Virus | Nef | Endocytosis of MHC-1 and CD4 |
| | Tat | Repression of MHC-1 gene promoter |
| | Vpu | Destabilization of newly synthesized MHC-1 |
| | Unknown | Inhibition of TAP |
| Human Papilloma Virus | E7 | Repression of MHC-1 gene promoter, repression of TAP gene promoter |
| Herpes Simplex Virus | ICP-47 | Inhibition of TAP |
| Kaposi's Sarcoma Herpes Virus | K3<br>K5 | Targets MHC-1 for degradation |
| Murine Cytomegalovirus | gp37/40 | Retention of MHC in ER / Golgi |
| | gp48 | Targets MHC for degradation |
| Murine Herpes Virus | mK3 | Targets MHC-1 for degradation |
| Myxoma Virus | m153R | MHC-1 internalization and degradation |
| Porcine Reproductive and Respiratory Syndrome Virus | Unknown | Down regulation of MHC-1 expression |
| Vaccinia Virus | UL49.5 | Inhibition of TAP |

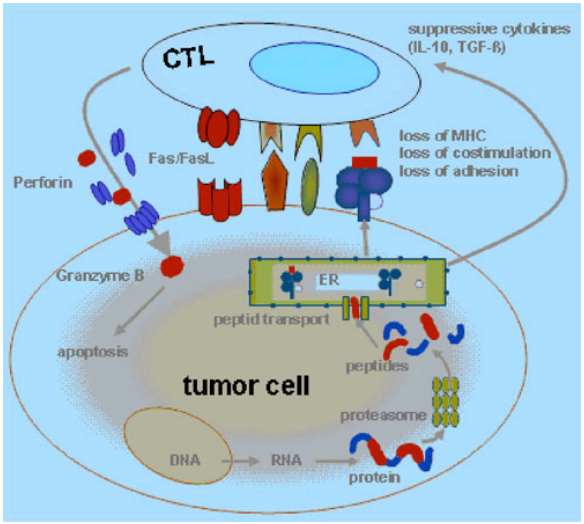


**Tumor escape from immune recognition: loss of HLA-A2 melanoma cell surface expression is associated with a complex rearrangement of the short arm of chromosome 6MJ Maeurer, MJ Maeurer et al;** Clinical Cancer Research, 1996

UPMC PARIS UNIVERSITAS

B. Bellier

# Importance des paramètres de fixation du TCR en fonction de la fréquence des complexes CMH-Ag

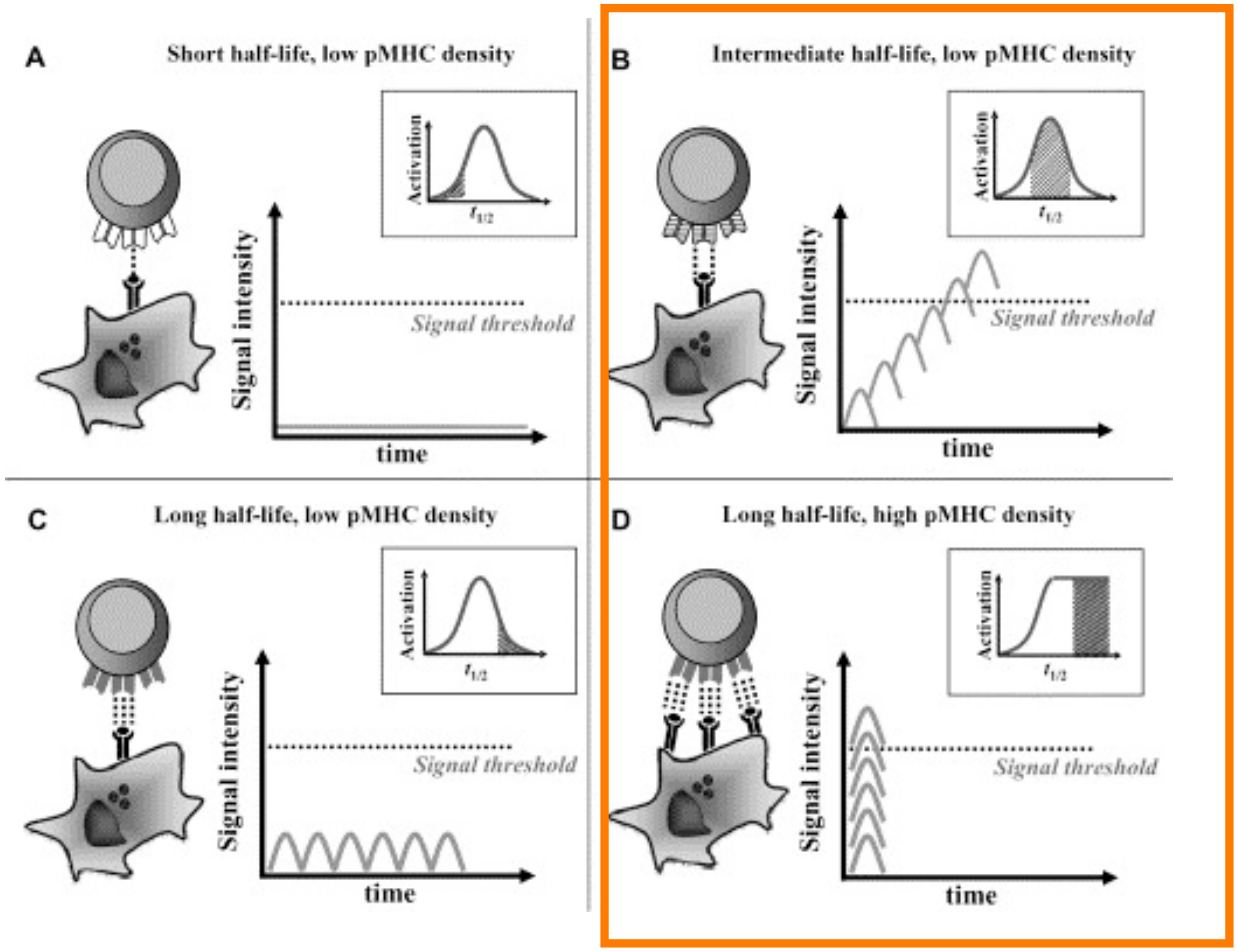


Sélection clonale: immunodominance

Importance de la sur-expression des molécules de CMH par les dendritiques après activation

The temporal TCR signal summation model suggests the existence of an optimal TCR/pMHC half-life for T cell activation in response to low-density cognate pMHC ligand. (A) TCR/pMHC interactions with short half-lives fail to activate the T cell (inset) in response to low-density pMHC due to summation of TCR signalling not reaching the activating threshold. (B) TCR/pMHC interactions with optimal half-life lead to efficient T cell activation (inset) as a result of summation of productive TCR signalling that reaches the activating threshold. (C) TCR/pMHC interactions with prolonged half-lives fail to activate T cells (inset) in response to low-density pMHC, due to TCR signals being generated at low frequency (TCR serial engagement blockade) and fail to be added one over the other due to intrinsic signal decay. Thus, T cell activation is impaired (inset) as activating threshold is not reached. (D) However, TCR/pMHC interactions with prolonged half-life can lead to T cell activation (inset) in response to high pMHC-density on the APC, because multiple productive TCR signals are generated simultaneously. These signals can be added and the T cell activation threshold reached.

# Paramètres quantitatifs de l'activation

$10^5$ TCR / T

Engagement de
3 à 400 TCR différents

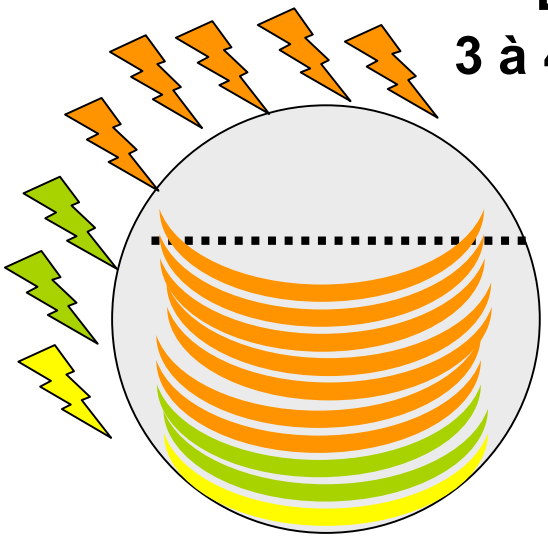

x 1- 200 / t = 2 - 30 s

Dépend de la présence de

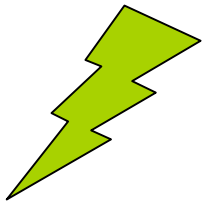

CD8

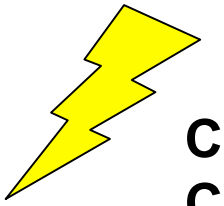

CD28
CD40L

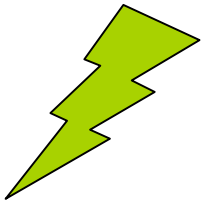

LFA-1

# Rôle des molécules adaptatrices et de costimulation

- **Molécules adaptatrices:**
  - Stabilisation de l'interaction TCR/CMH
  - Modèles d'initiation de l'activation
- **Molécules de costimulation:**
  - Transduction du signal : **renforcement des voies de signalisation**

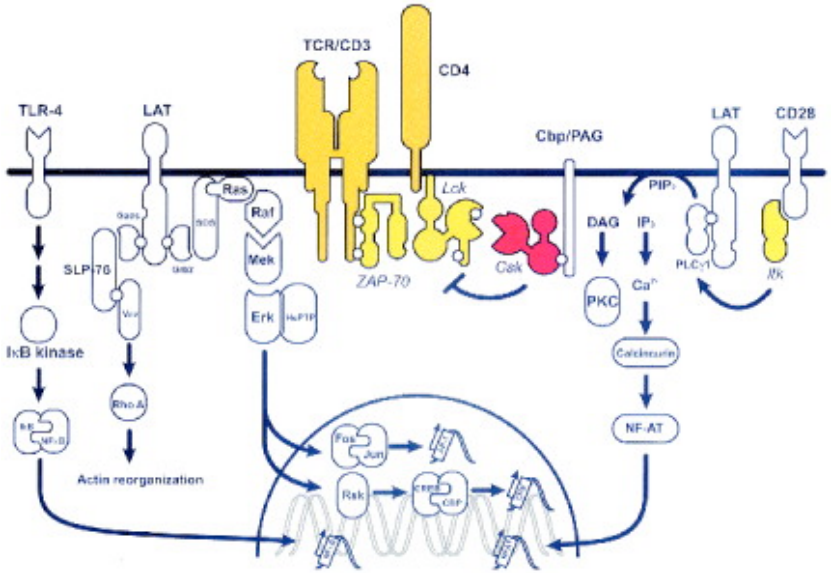


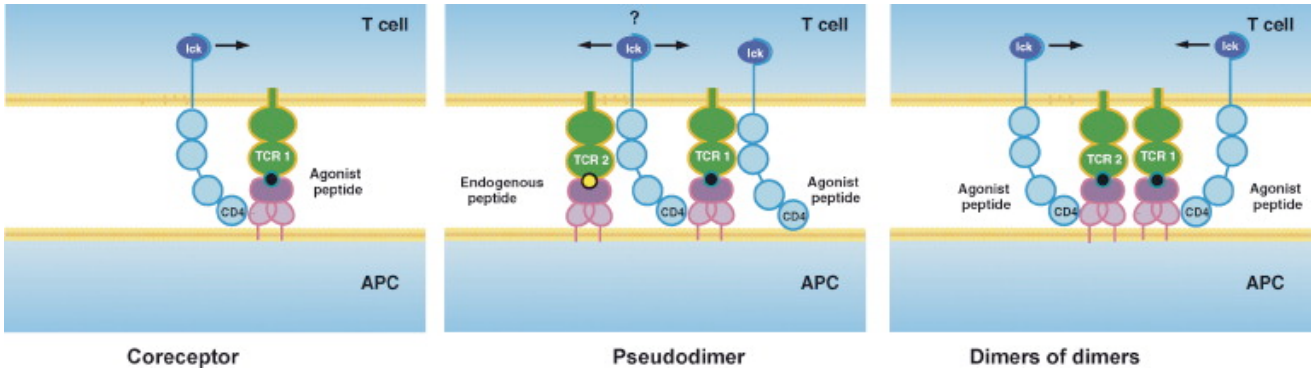


*Michelle Krogsgaard, Sim Imm 2007*

UPMC PARIS UNIVERSITAS

B. Bellier

# Rôle des molécules adaptatrices : CD8

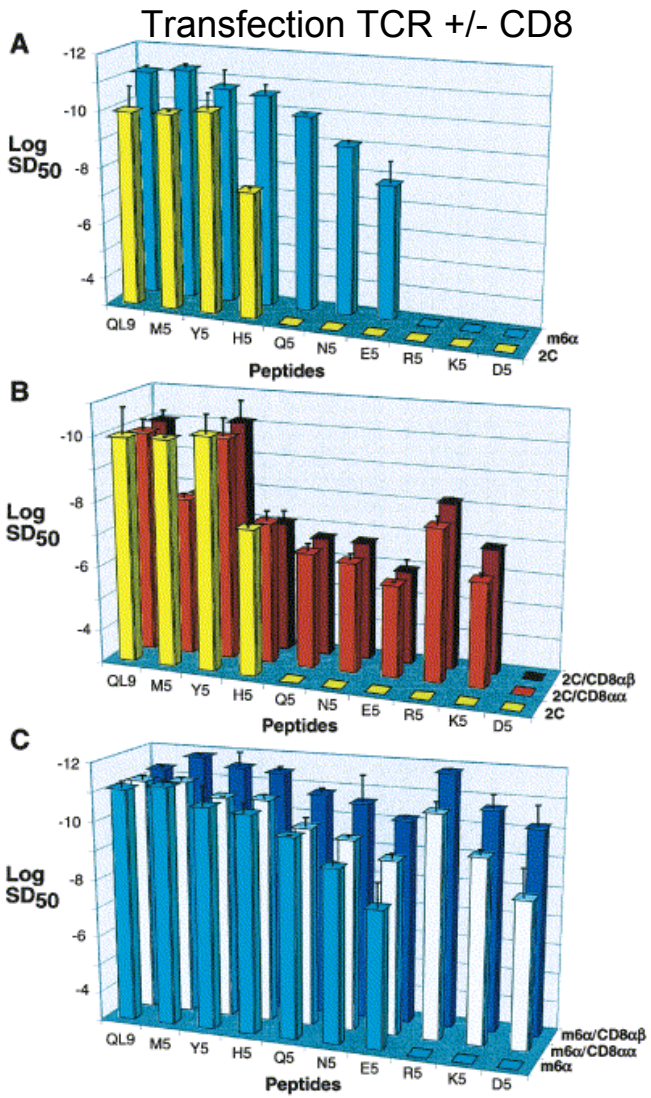


***Holler D , Imm 2003***

The αβ-negative T cell hybridoma 58-/- was cotransfected with the 2C wt α chain gene and one of five different α chain genes from 2C and the mutants m6α m13α m33α and m67α . Stable transfectants that expressed similar levels of TCR were identified based on their staining with anti-Vα antibody KJ16

Sensitization Doses of Various QL9 Position 5 Variant PeptidesIL-2 production by transfectants stimulated with various peptides was measured as described in the Experimental Procedures. The amount of peptide that yielded 50% of the maximum IL-2 release (SD50) was calculated by linear regression of IL-2 curves (see Figure S1 at http://www.immunity.com.gate1.inist.fr/cgi/content/full/18/2/255/DC1). The log of the SD50 value was plotted for each of the peptides used to stimulate transfectants: (A) 2C and m6_ CD8-negative; (B) 2C CD8-negative, 2C/CD8__ and 2C/CD8__ (C) m6_CD8-negative, m6_CD8__ and m6_CD8__ In Figure 3, Figure 4 and Figure 5, log SD50 values represent the mean of at least two assays. Error bars indicating one standard deviation are included for each point (for some points these error bars are not apparent as they are smaller than the size of the symbol).

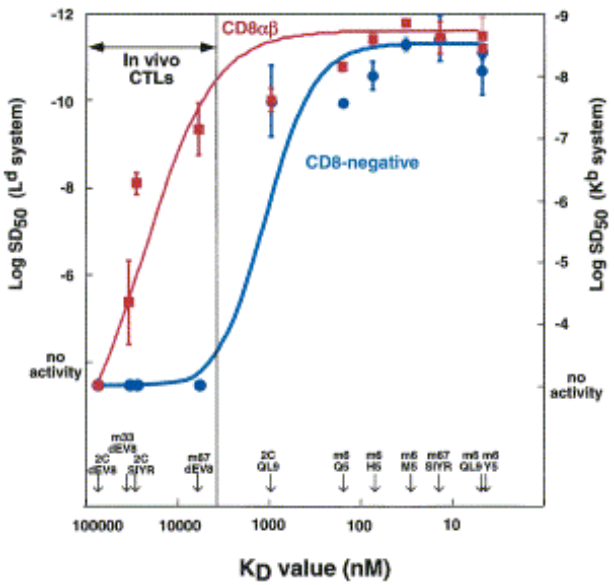


Relationship of Peptide Activity and TCR:pepMHC Affinity. SD50 values of various peptides were plotted versus the equilibrium affinity constants (KD) of the corresponding TCR:pepMHC interaction (Table 1). In order to include values from the Ld and Kb systems, SD50 values from the two different antigen-presenting cell systems (T2-Ld and T2-Kb) are shown on the two Y-axes. The points represent data derived from CD8-negative transfectants (blue circles) and CD8__transfectants (red squares) of the corresponding TCR transfectant. The corresponding TCR/pepMHC interactions are shown at the bottom of the figure. The range of KD values that correspond to affinities measured for known TCR:syngeneic MHC interactions from in vivo CTLs are shown. This range falls exclusively in the CD8-dependent category, as determined by TCR-transfection studies (not necessarily anti-CD8 antibody inhibition studies).

**The significant enhancement in recognition of the peptides could be improved by one to two orders of magnitude by the introduction of CD8 into transfectants**

# Molécule adaptatrices: indépendance pour les TCR de haute affinité

Kerry JI 2003

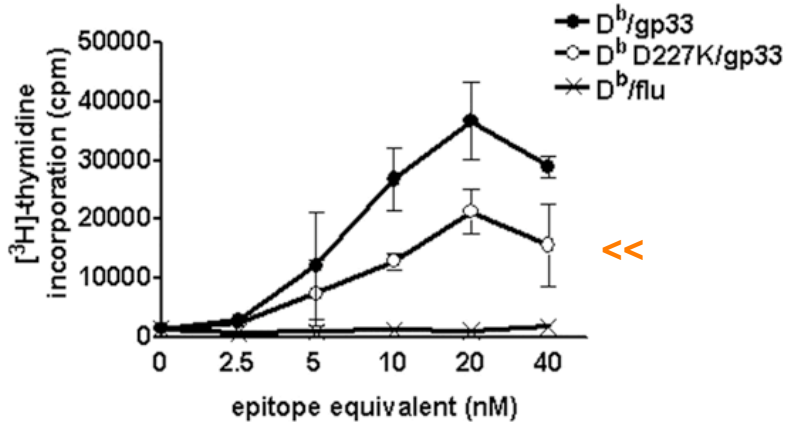


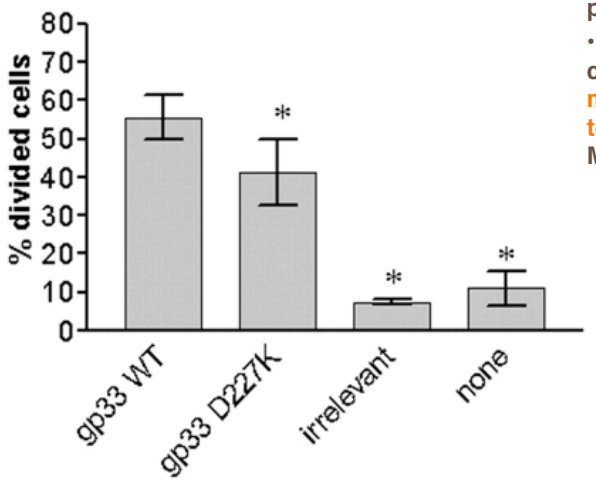


- Model:
- TCR-transgenic CD8 (P14)
- GP33 (KAVYNFATC) ou C9M (KAVYNFATM; affinity >) peptides presented by
- H-2Db tetamers or tetramers containing the $D^b$ D227K mutation, which has been shown to abrogate CD8 interaction with MHC

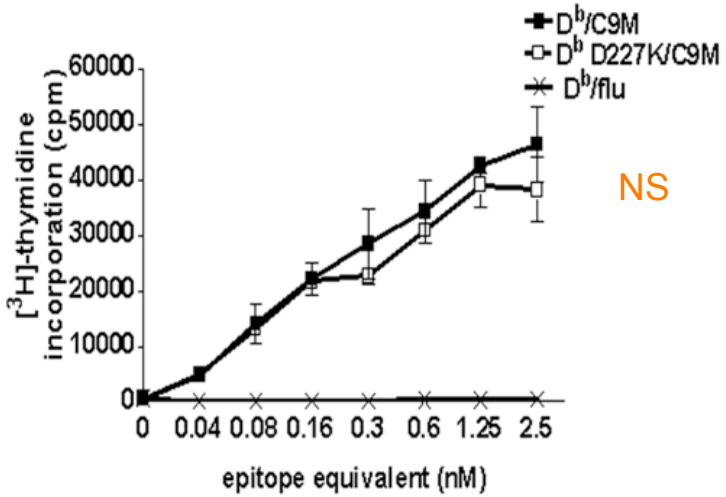


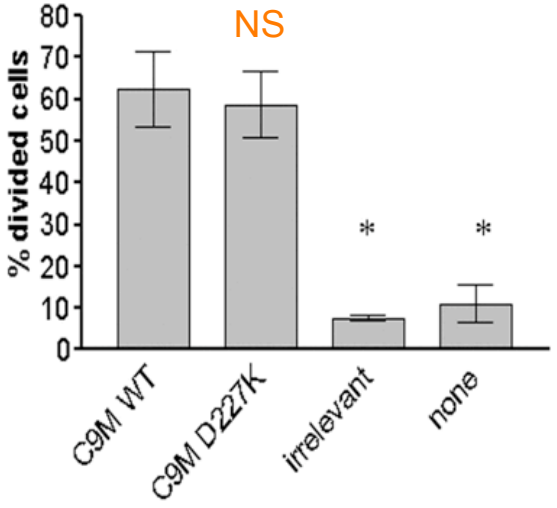

# Costimulation / anergie

- **Absence:**
  - mécanisme de tolérance périphérique: ignorance immunologique
  - Induction d'anergie

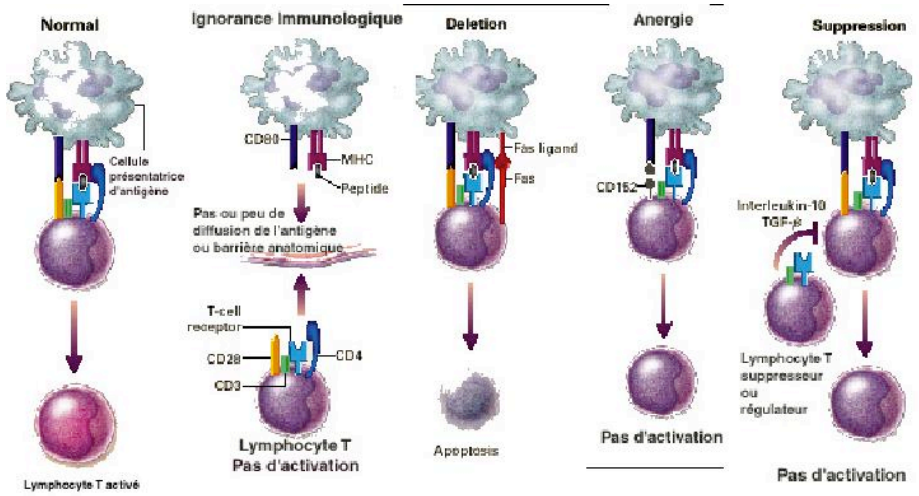


- **Mol de costimulation: signal complémentaire**

Mécanismes possibles de la tolérance périphérique

Figure N°22

New England J Med 2001, 344, 65

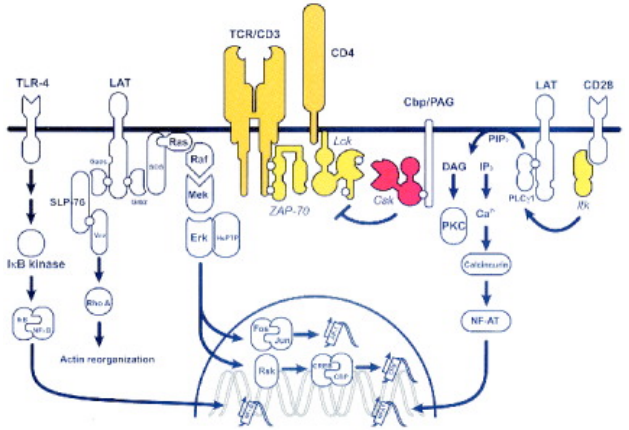

# Nécessité d'un engagement prolongé de CD80/CD86

*Liwski, Imm Letters 2006*

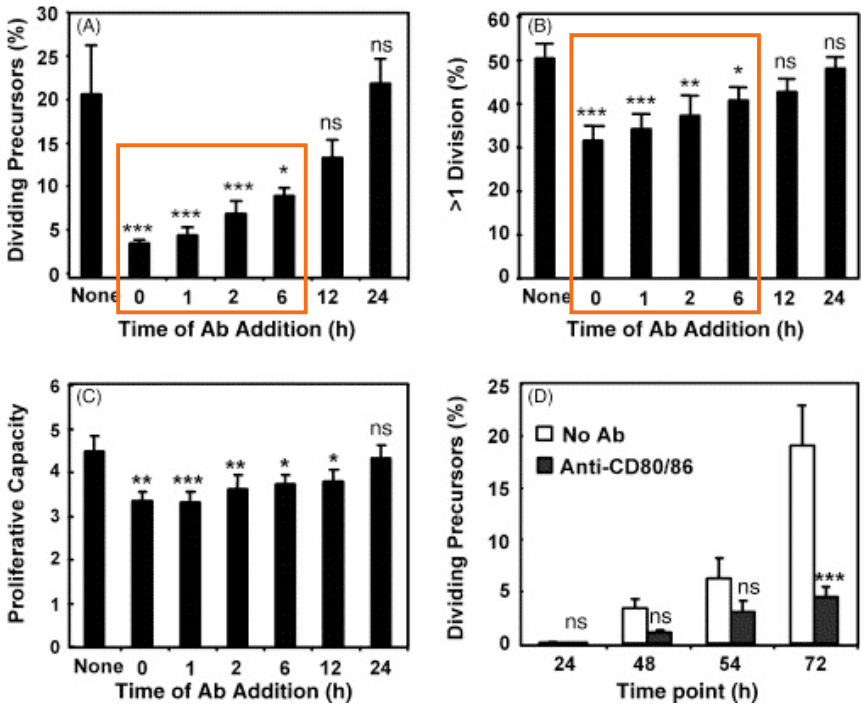


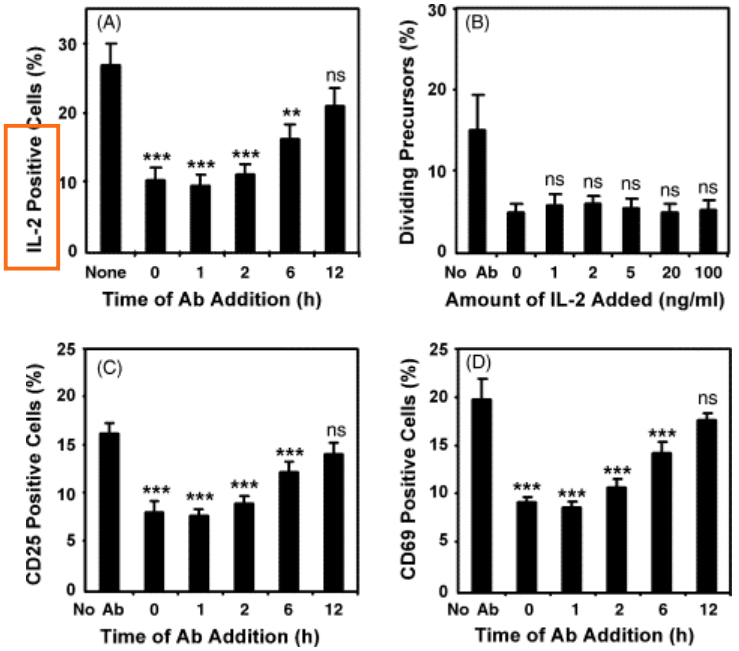


- To investigate the functional effects of CD80/CD86 blockade on naive CD4+ T cell activation, freshly isolated CD4+ T cells from OVA-TCR transgenic DO11.10 mice [27] were labeled with CFSE and cultured with OVA-peptide pulsed, mature DC in the absence or presence of CD80 and CD86 specific mAbs.

- We demonstrated that DC mediated CD80/CD86 costimulation controls the magnitude of the naïve T cell proliferative response by regulating both responder frequency as well as proliferative capacity.

- Our data revealed that blocking CD80/CD86 signaling up to 6 h after conjugate formation resulted in a significant decrease in both the number of naive T cells entering the proliferative cycle and the number of daughter cells generated by each cell.

# Mol costimulation et dynamique de l'interaction

- *Federica Benvenuti, JI 2004;* Dendritic Cell Maturation Controls Adhesion, Synapse Formation, and the Duration of the Interactions with Naive T Lymphocytes

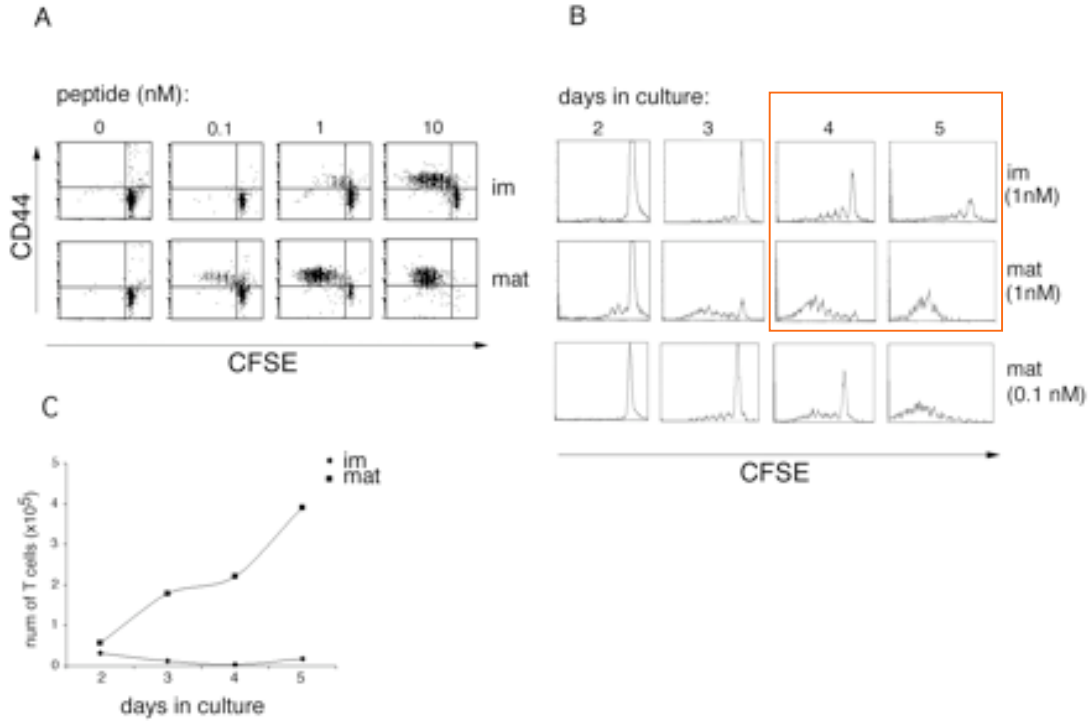


- Proliferation of naive T cells stimulated by **immature or mature DCs**. Immature or mature D1 pulsed with different doses of peptide were cocultured for 5 days with CFSE-loaded naive T lymphocytes (1:5 ratio). *A*, Representative dot blot profile showing the loss of CFSE and the up-regulation of CD44 induced by immature (*upper row*) or mature (*lower row*) DCs loaded with different peptide doses at day 3. *B*, Histogram profile of CFSE staining on naive T cells stimulated with immature (*upper row*) or mature (*middle row*) DCs loaded with 1 nM H-Y and mature DCs loaded with 0.1 nM peptide (*lower row*) at days 2–5 of the coculture. *C*, Quantification of the absolute number of CD4+ T cells at the different days of coculture for immature () and mature () DCs loaded with 1 nM peptide (T cells at day 0 = 7 x 104). One representative of three experiments is shown.

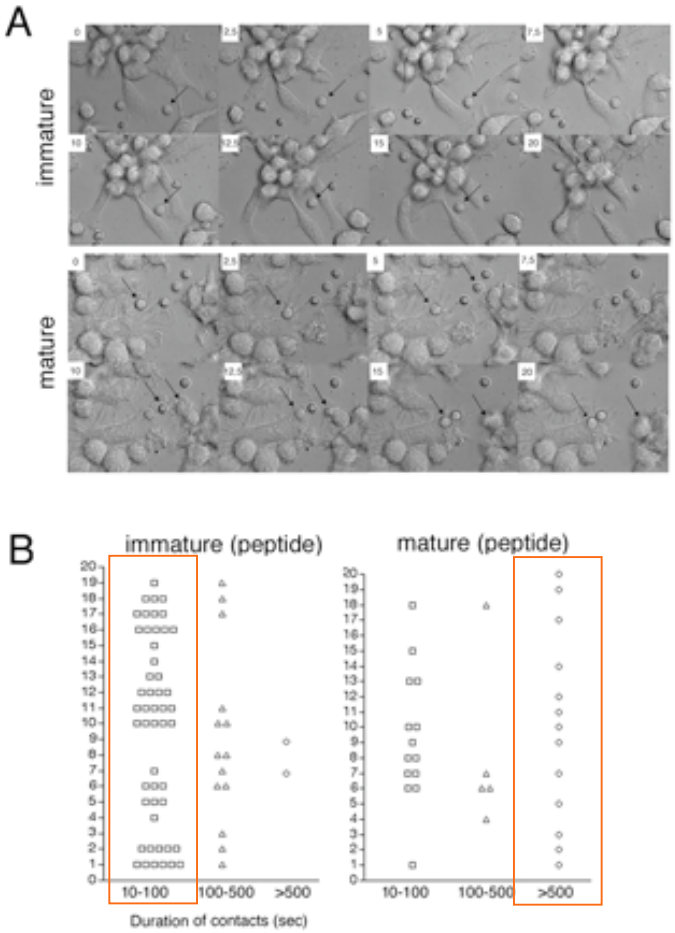

# Mol de costimulation et synapse

- *Federica Benvenuti, JI 2004;* Dendritic Cell Maturation Controls Adhesion, Synapse Formation, and the Duration of the Interactions with Naive T Lymphocytes

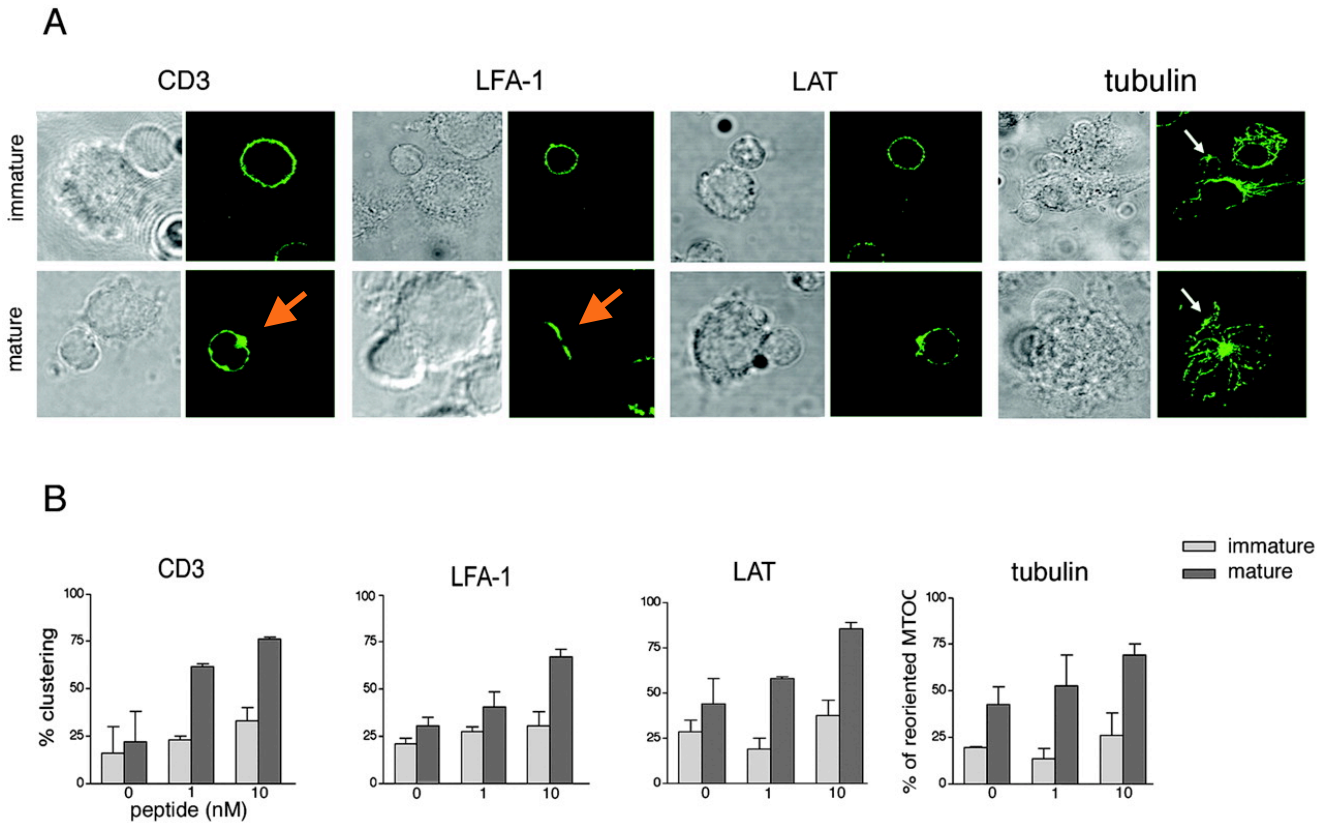


## *DC maturation is required for effective clustering and SMAC formation at the DC-T cell contact site*

Efficient clustering in naive T cells requires DC maturation. Confocal images showing the distribution of CD3, LFA-1, LAT, and tubulin in T cells forming conjugates with immature or mature D1 pulsed with 10 nM H-Y peptide. Conjugates were formed for 30 min, washed five times, and fixed for immunostaining. *A*, One representative conjugate formed with immature DCs (*upper panels*) or mature DCs (*lower panels*) is shown for each marker. For each immunofluorescent image (*right panels*), a DIC image showing the two cells in contact is shown (*left panels*). Note that the distribution of CD3, LFA-1, and LAT is homogenous on T cells forming conjugates with immature DCs and clustered in conjugates formed with mature DCs. Similarly, the T cell MTOC (marked by an arrow) is reoriented toward the APCs in conjugates with mature, but not with immature DCs. *B*, Quantification of the proportion of conjugates showing clustering of CD3, LFA-1, LAT, and tubulin at the site of contact. Conjugates between naive T cells and immature or mature DCs pulsed with different doses of H-Y peptide were formed as in *A*. The number of conjugates presenting clustering at the contact zone was blindly quantified (see *Materials and Methods*) and expressed as a percentage of the total number of conjugates analyzed (percent clustering). Number of conjugates quantified is as follows: CD3, immature, $n = 276$; mature, $n = 347$; LFA-1, immature, $n = 197$; mature, $n = 229$; LAT, immature, $n = 185$; mature, $n = 232$; and tubulin, immature, $n = 210$; mature, $n = 243$.

B. Bellier

# Conséquence des interactions T sur la différenciation T

# Génération des CD8 mémoire: Influence de la quantité d'Ag

- *E. John Wherry, JI* 2002, Generation of CD8+ T Cell Memory in Response to Low, High, and Excessive Levels of Epitope

Table I. *VV recombinants*

| Recombinant | Description | Epitopes/Cell[a] (copies/cell) |
|---|---|---|
| M50 | Control virus-expressing an irrelevant minigene ($NP_{50-57}$; H-$2K^b$) | 0 |
| HP19 | Full-length NP/S (influenza NP + SIINFEKL) behind a 19bp HP | ~800 |
| HP0 | Full-length NP/S (influenza NP + SIINFEKL) without a HP (HP size = 0) | ~30,000 |
| (M)SIINFEKL | Minigene version of $OVA_{257-264}$ (M designates the initiating methionine) | ~60,000 |

Espaceur:
< expresion
de l'Ag

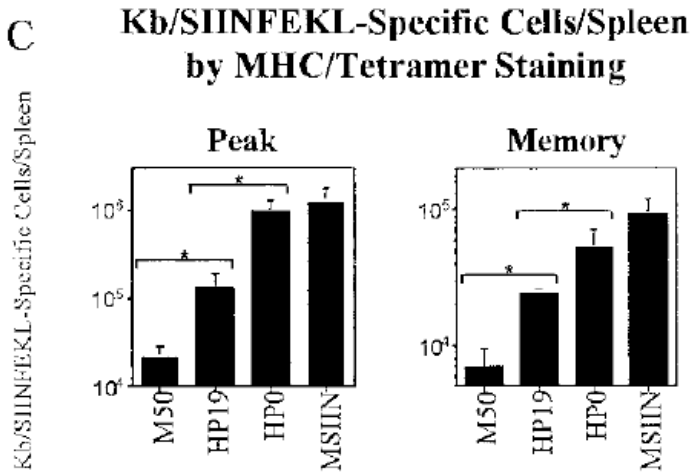


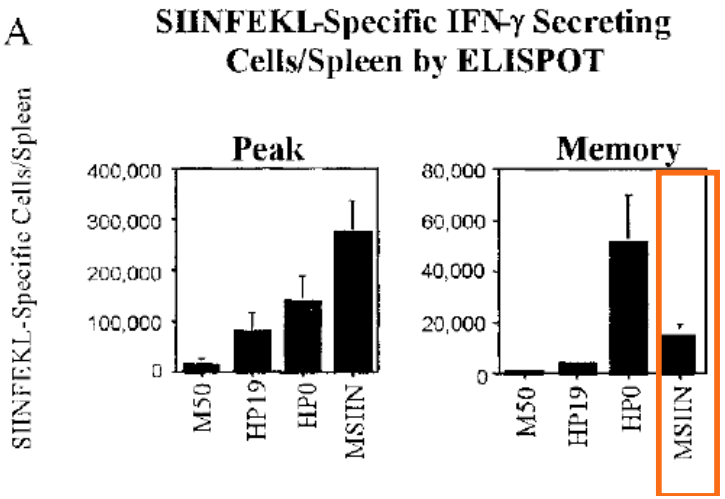


➢**recrutement d'un nombre de clones plus ou moins important**

➢**et d'affinité variable**

**selon quantité d'Ag lors de la stimulation**

# Importance des paramètres d'activation : Génération des CD8 mémoire

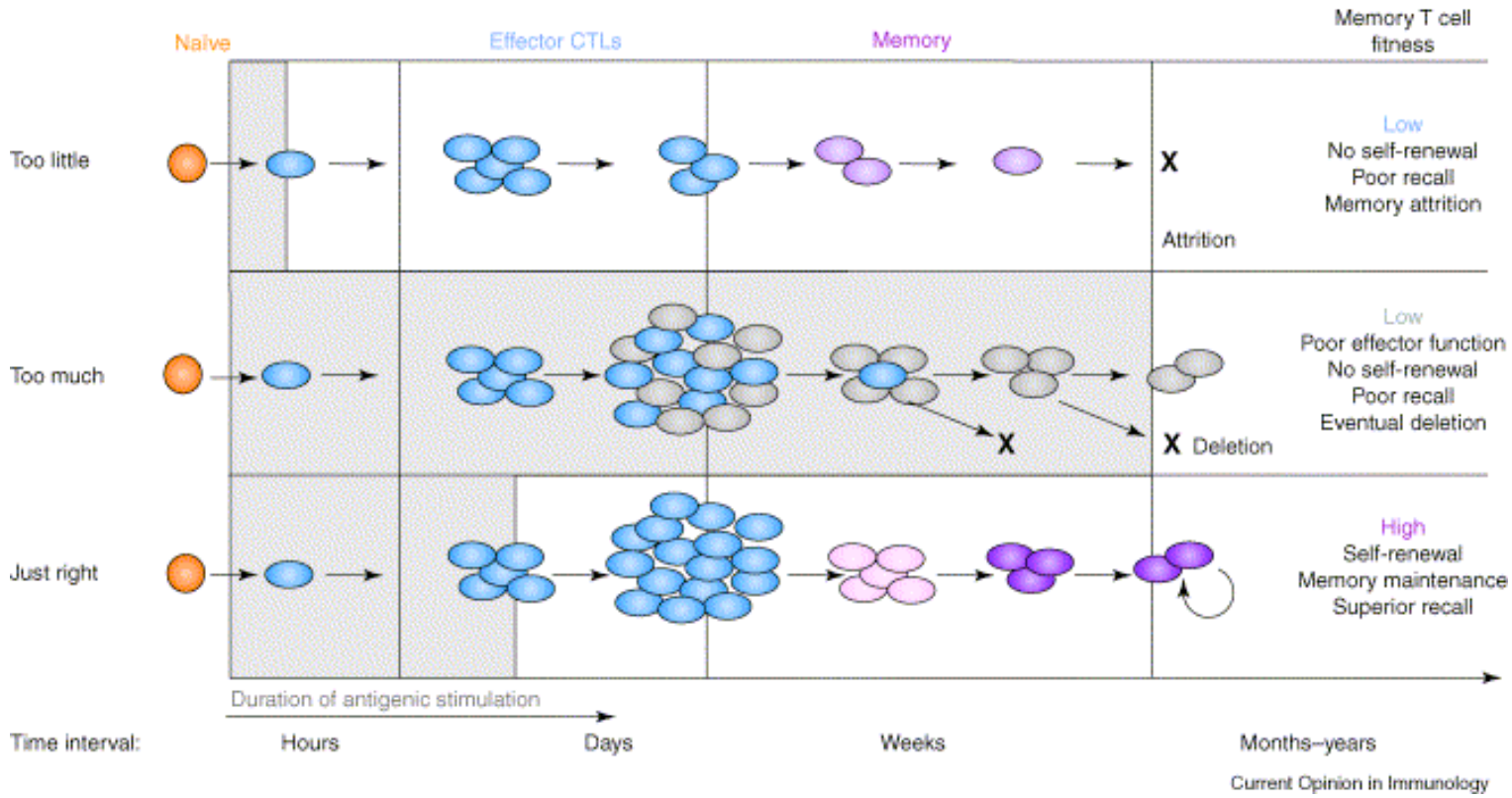


*Masopust Curr Op Imm 2004*

The Goldilocks model of effector and memory CD8+ T-cell development. The first 24 hours following antigenic stimulation elicits a program of expansion and differentiation that continues among daughter cells after removal of antigen. 'Too little' stimulation, meaning insufficient antigen concentration or duration, leads to limited CD8+ T-cell expansion, poor memory development and attrition. Chronic antigen exposure may cause 'too much' stimulation, leading to a progressive loss in the ability to secrete cytokines and the eventual deletion of antigen-specific CD8+ T cells. Optimum memory development is favored when conditions are 'just right'; that is, when CD8+ T cells are stimulated by a sufficient concentration of antigen for a sufficient, but not excessive period of time. Several variables, such as the cytokine environment, TCR affinity, type of antigen presenting cells, CD4+ T-cell help and degree of co-stimulation, modify the differentiation program and alter the antigen-dependent signaling requirements for the development of a robust response. Several factors encountered during the days following priming, including continued antigen contact, various co-stimulatory molecules, negative regulators, cytokines, chemokines, CD4+ T-cell help and anatomical location might also have a large qualitative and quantitative influence on the developing response. Additional factors may be important weeks and months later for memory differentiation and maintenance.

# Prolongation de la stimulation antigénique: conséquence sur la différenciation en cellules mémoire

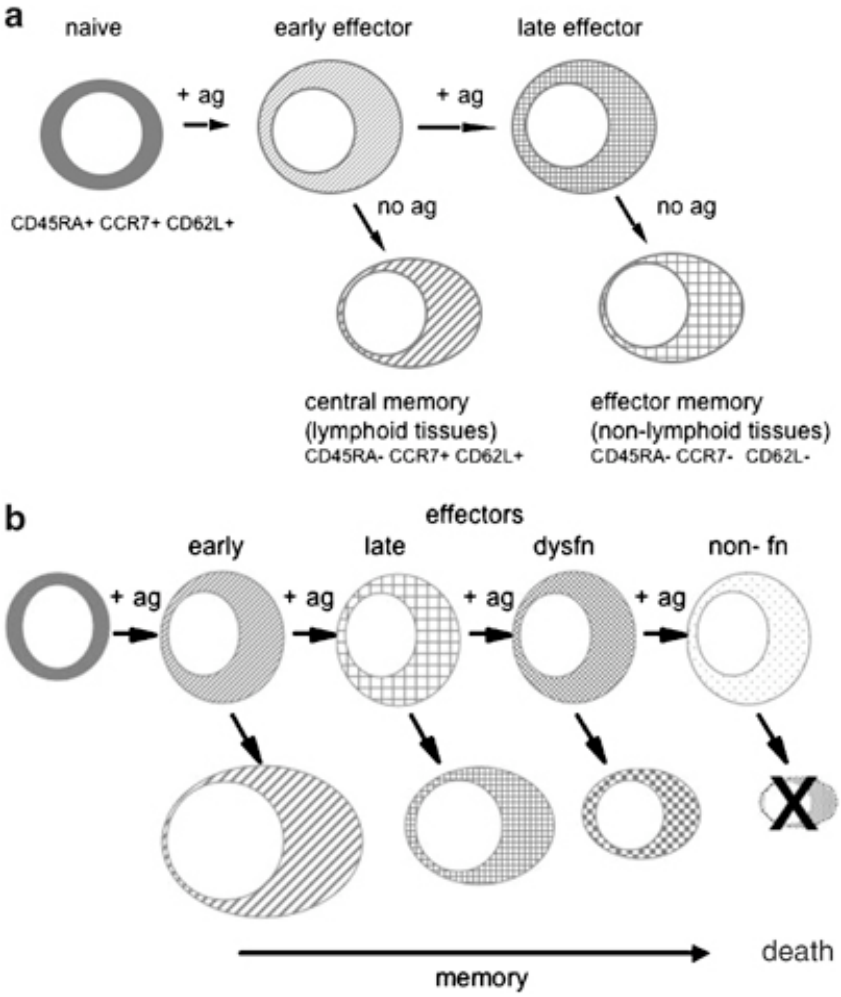


M L Munier and A D Kelleher

# Importance de la stimulation antigénique initiale: programme de différenciation

- Susan M. Kaech & Rafi Ahmed *Nature Immunology* 2001 ; Memory CD8+ T cell differentiation: initial antigen encounter triggers a developmental program in naïve cells

- **Models for proliferation and differentiation of naïve CD8+ T cells.**(**a**) CD8+ T cell proliferation is dependent on repeated encounters with antigen. Each cell that is stimulated by antigen divides and progressively differentiates into effector CTLs and memory CD8+ T cells with each successive cell division. According to this model, it is essential that each daughter cell be stimulated with antigen, otherwise CD8+ T cell division, and possibly differentiation, would be halted upon antigen removal. (**b**) **Naïve CD8+ T cells are developmentally programmed to divide at least seven to ten times and to differentiate into effector CTLs and long-lived functional memory CD8+ T cells.** Optimal antigenic stimulation of the parental cell triggers this developmental program and the CD8+ T cells become committed to proliferation and differentiation. Further antigenic stimulation of the daughter cells may increase the number of times the activated CD8+ T cells divide, but it is unnecessary for this developmental program to progress.

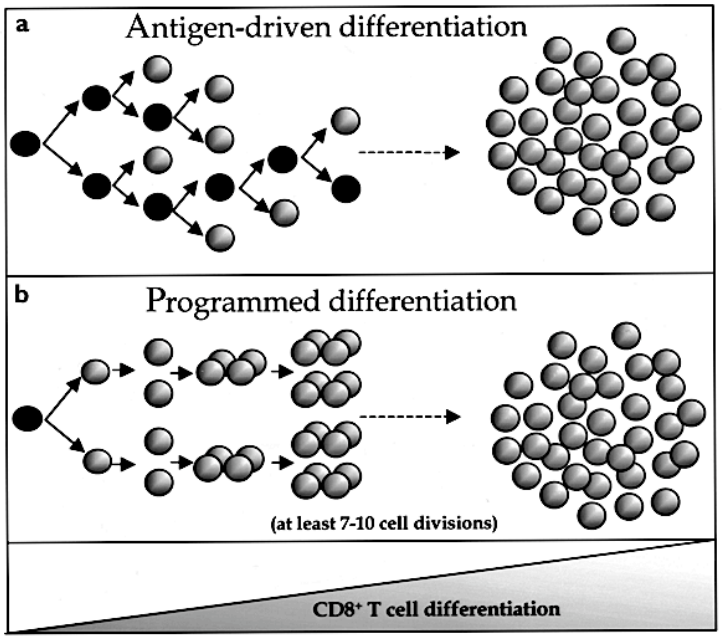

# Selective expression of the interleukin 7 receptor identifies effector CD8 T cells that give rise to long-lived memory cells

*Kaech, Nat Immunol 2003*

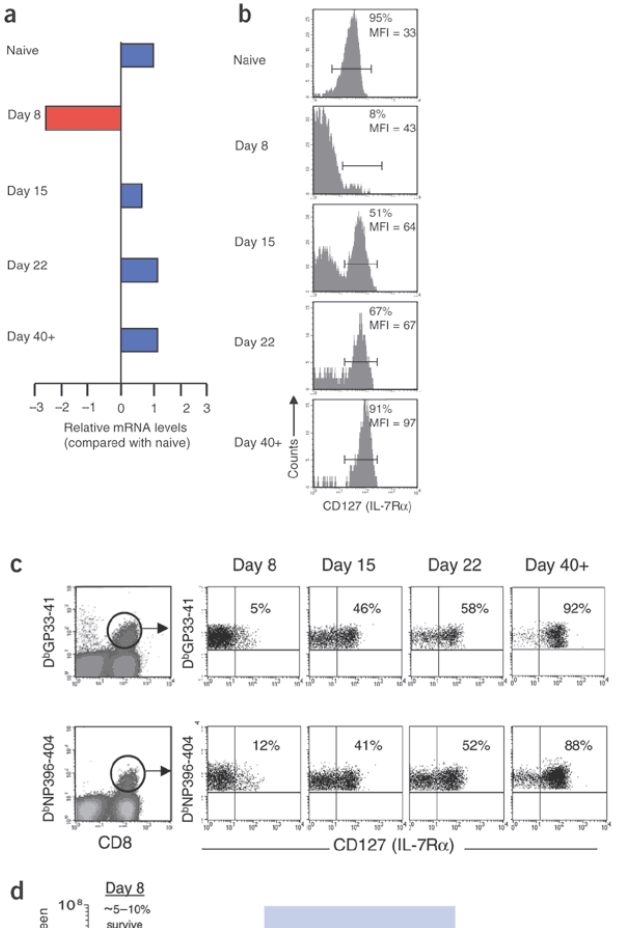


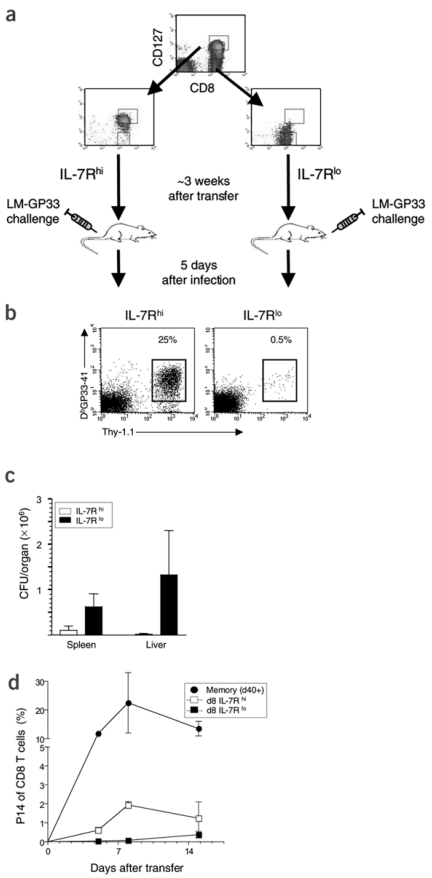


**IL-7R$^{hi}$ memory cell precursors provide immunological protection.** (**a**_) IL-7R$^{hi}$ or IL-7R$^{lo}$ Thy-1.1$^{+}$ P14 effector cells (2 10$^{5}$) from day 11 were adoptively transferred into naive hosts, and 3 weeks later the mice were infected with 5 10$^{4}$ CFU of recombinant *L. monocytogenes* expressing the GP33-41 epitope (LM-GP33). Mice were examined 5 d later. (**b**) Donor Thy-1.1$^{+}$ P14 cell population expansion. Dot plots gated on CD8 T cells; percents indicate Thy-1.1$^{+}$ P14 cells in the spleen. (**c**) Bacterial clearance. Bacterial titers were measured in spleen and liver. Similar results were obtained in separate experiments in which IL-7R$^{hi}$ and IL-7R$^{lo}$ effector cells from day 15 were transferred. (**d**) Equal numbers (0.8 10$^{6}$) of IL-7R$^{hi}$ or IL-7R$^{lo}$ effector Thy-1.1$^{+}$ P14 CD8 T cells from day 8 after infection (d8) or memory Thy-1.1$^{+}$ P14 CD8 T cells from day 40 or later after infection (d40+) were transferred into mice persistently infected with LCMV, and their ability to proliferate *in vivo* after antigenic stimulation was assessed. Data represent percentage of donor Thy-1.1$^{+}$ P14 cells of total CD8 T cells in the blood on days 5, 8 and 15 after transfer.

- **Increased expression of IL-7R directly correlates with effector CD8 T cell survival.** (**a**) Differential expression of IL-7R mRNA in naive, effector and memory P14 CD8 T cells. Expression of IL-7R mRNA was measured by DNA microarray analysis in P14 CD8 T cells from days 8, 15, 22 and >40 after LCMV infection and was compared with that of naive P14 CD8 T cells. Bars represent the relative fold difference based on a $\log_2$ scale. The P14 CD8 T cells express a transgenic TCR that recognizes the gp33-41 epitope of LCMV. (**b**) Cell surface IL-7R expression on naive P14 CD8 T cells or P14 CD8 T cells from days 8, 15, 22 and 40 after infection. The percent and mean fluorescent intensity (MFI) of bracketed IL-7R$^{hi}$ cells are given. (**c**) C57BL/6 mice were infected with LCMV, and 8, 15, 22 and >40 d after infection, the cell surface expression of IL-7R on D$^{b}$GP33-41- and D$^{b}$NP396-404-specific CD8 T cells was assessed by staining with anti-CD8 and anti-IL-7R and either D$^{b}$GP33-41 or D$^{b}$NP396-404 major histocompatibility complex class I tetramers. The dot plots are gated on tetramer-positive CD8 T cells, and the percent of IL-7R$^{hi}$ cells is indicated. Circles and arrows indicate the source of cells in dot plots to the right. (**d**) LCMV-specific CD8 T cells in the spleen 8, 15, 22 and >40 days after infection were quantified by major histocompatibility complex class I tetramer staining as well as by intracellular cytokine staining for IFN- after 5 h of stimulation with LCMV peptides. The percent of LCMV-specific CD8 T cells predicted to survive at day 8, 15, 22 and approximately 40 after infection was calculated by dividing the number of LCMV-specific memory CD8 T cells (at day 40 or more after infection) by the number of virus-specific CD8 T cells at each time point. (**e**) C57BL/6 (Thy-1.2$^{+}$) mice containing 1 10$^{4}$ naive TCR-transgenic CD8 T cells from Thy-1.1$^{+}$ P14 mice that recognize the LCMV epitope GP33-41 were infected with LCMV, and 8 d later the expression of granzyme B, CD62L, CD43, CD27 and KLRG-1 was compared between IL-7R$^{hi}$ (blue) and IL-7R$^{lo}$ (red) Thy-1.1$^{+}$ effector cells and naive CD8 T cells (black). Arrow indicates the source of cells in histograms.

UPMC PARIS UNIVERSITAS
B. Bellier

# Functional and genomic profiling of effector CD8 T cell subsets with distinct memory fates

*Sarkar S et al, JExpMed 2008*

**Effector CD8 T cells uniformly down-regulate CD127 but can be distinguished on the basis of KLRG-1 expression.** (A) Cell-surface expression of IL-7R_with respect to cell division at days 1ñ4 after LCMV infection. $10^6$ naive CFSE-labeled P14 CD8 T cells were adoptively transferred into naive mice that were subsequently infected with LCMV. All plots are gated on $CD8^+$ $Thy1.1^+$ P14 splenocytes directly stained ex vivo for IL-7R_expression. An uninfected naive control is also shown, and the red horizontal line indicates the naive level of expression. (B) Phenotypic properties of $CD127^{Lo}$ antigen-specific cells at day 4.5 p.i. B6 mice containing ~$10^5$ naive $Thy1.1^+$ P14 cells were infected with LCMV, and expression of the indicated cell-surface and intracellular markers on $CD8^+$ $Thy1.1^+$ splenocytes was assessed 4.5 d later (red line histograms). Gray histograms represent naive cells from uninfected control mice. (C) Longitudinal analysis of cell-surface IL-7R_and KLRG-1 expression. B6 mice containing ~$10^5$ naive $Thy1.1^+$ P14 cells were infected with LCMV, and the cell-surface expression of IL-7R_and KLRG-1 was analyzed at the indicated time points. Histograms depict the MFI of IL-7R_expression and percentages of $KLRG\text{-}1^{Hi}$ cells gated on $CD8^+$ $Thy1.1^+$ P14 cells. (D) Inverse association of KLRG-1 expression with the memory markers CD127 and CD62L. B6 mice containing $10^5$ $CD8^+$ $Thy1.1^+$ P14 cells were infected with LCMV, and KLRG-1 expression with respect to CD127 or CD62L was analyzed at the indicated time points.

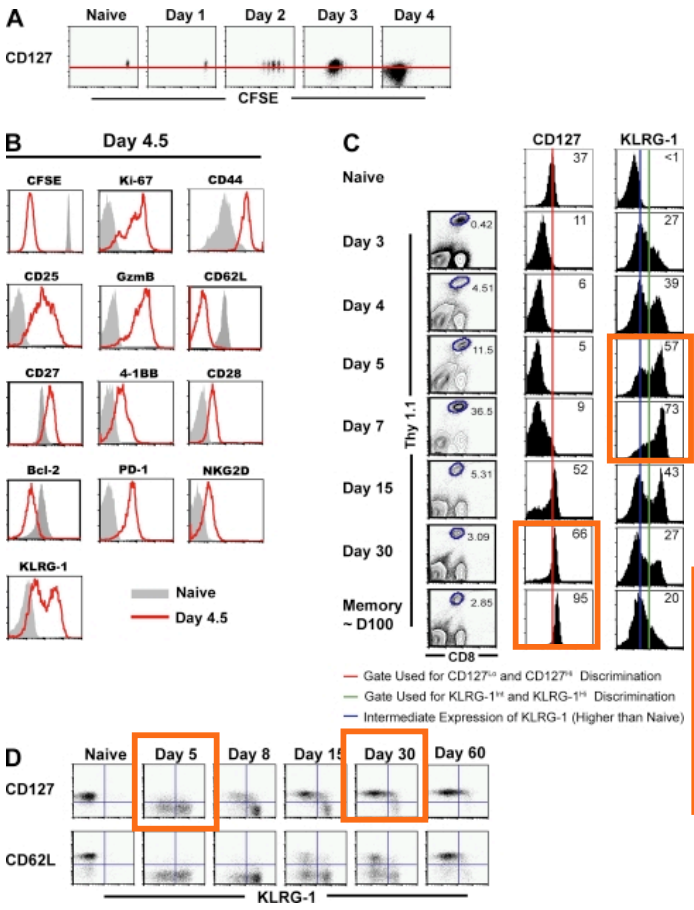


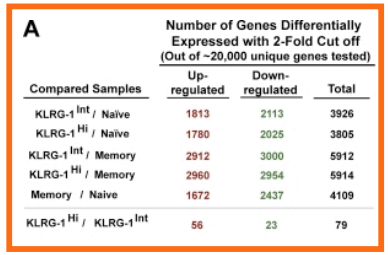

A

| Compared Samples | Number of Genes Differentially Expressed with 2-Fold Cut off (Out of ~20,000 unique genes tested) Up-regulated | Down-regulated | Total |
|---|---|---|---|
| $KLRG\text{-}1^{Int}$ / Naive | 1813 | 2113 | 3926 |
| $KLRG\text{-}1^{Hi}$ / Naive | 1780 | 2025 | 3805 |
| $KLRG\text{-}1^{Int}$ / Memory | 2912 | 3000 | 5912 |
| $KLRG\text{-}1^{Hi}$ / Memory | 2960 | 2954 | 5914 |
| Memory / Naive | 1672 | 2437 | 4109 |
| $KLRG\text{-}1^{Hi}$ / $KLRG\text{-}1^{Int}$ | 56 | 23 | 79 |

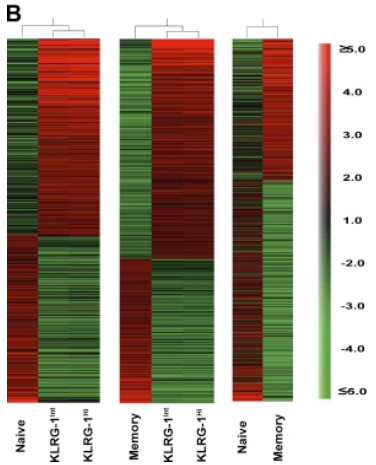


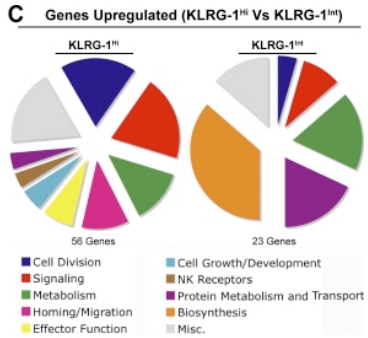


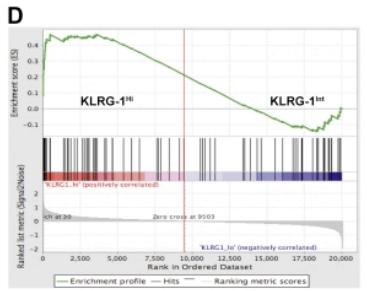

# Short effector / Memory precursor modulation by T-bet

**SLEC** KLRG1$^{hi}$ IL-7R$^{lo}$ **MPEC** KLRG1$^{hi}$ IL-7R$^{lo}$

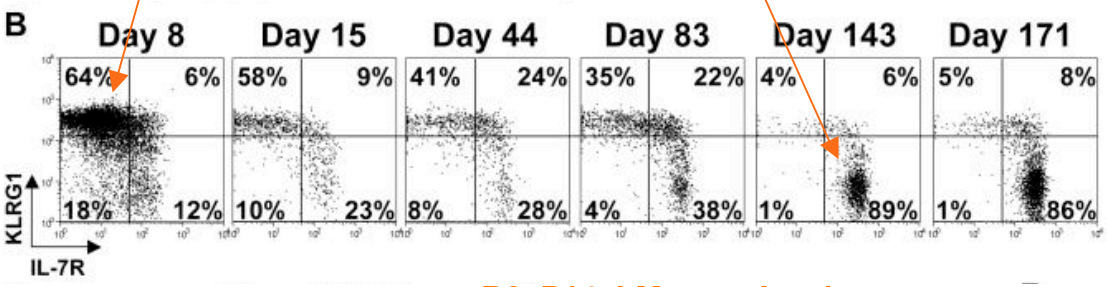


**Inflammation Directs Memory Precursor and Short-Lived Effector CD8(+) T Cell Fates via the Graded Expression of T-bet Transcription Factor**
***Joshi et al, Immunity 2007***

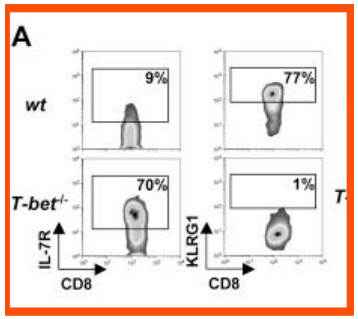


**T-bet expression is necessary and sufficient for development of KLRG1$^{hi}$ SLECs.**

**B6+P14+LM$_{GP33}$ ± Ampi**

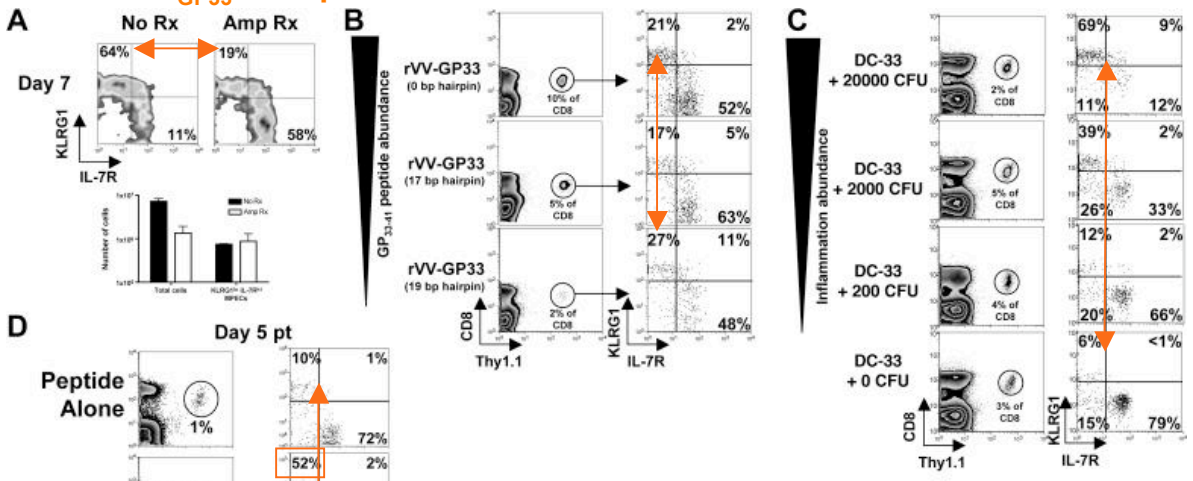


**Levels of inflammation regulate KLRG1$^{hi}$ IL-7R$^{lo}$ SLEC formation.**

UPMC PARIS UNIVERSITAS

B. Bellier

# Model of SLEC and MPEC development during acute viral infection.

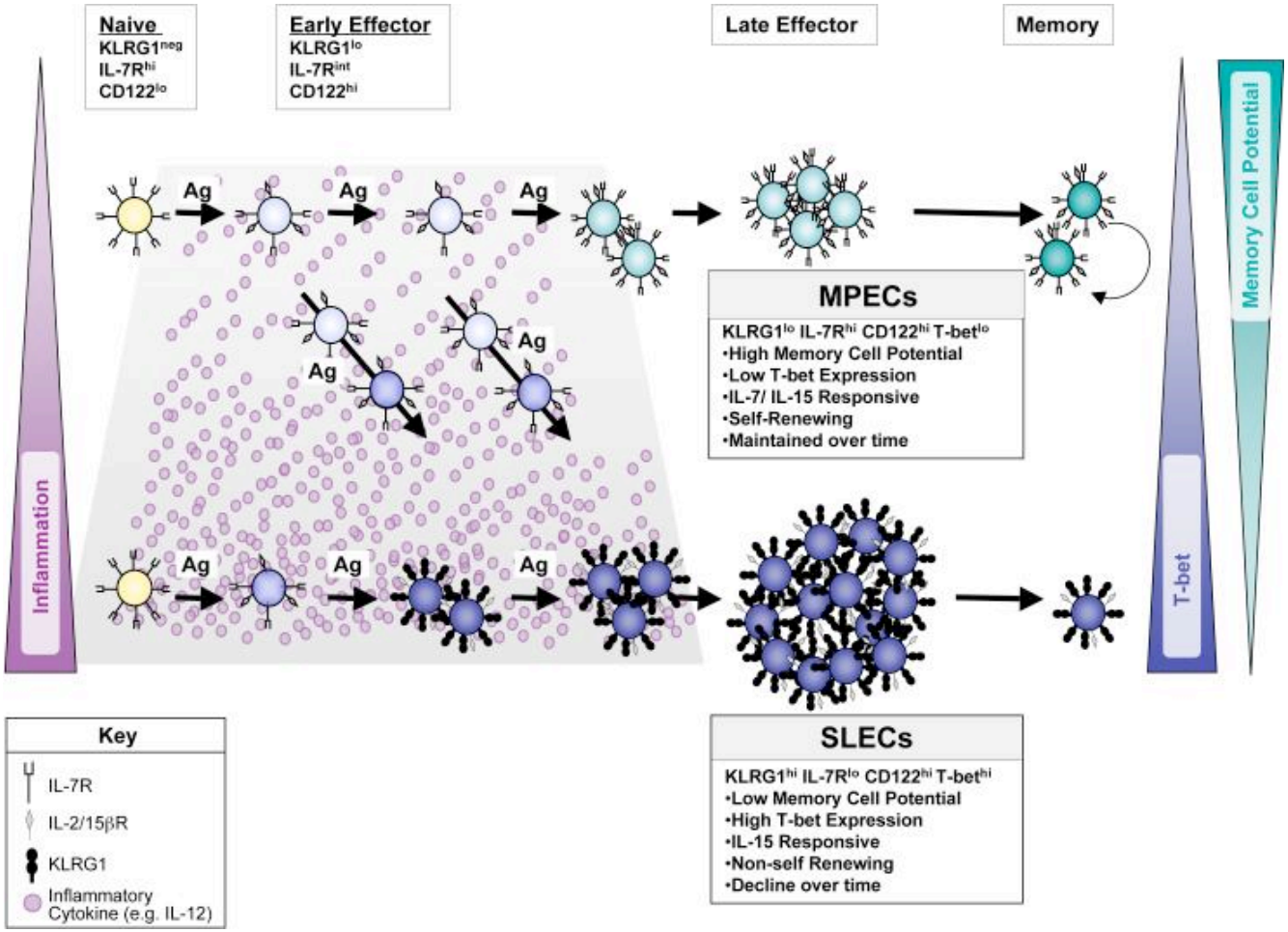


- Naive CD8 T cells are IL-7R$^{hi}$, CD122$^{lo}$ (IL-2/15_), KLRG1$^{neg}$ and T-bet$^{neg}$ and are IL-7 dependent. Early during infection, most effector CD8 T cells become CD122$^{hi}$ and downregulate IL-7R to an intermediate-to-low level, but expression of T-bet and KLRG1 is set depending on their exposure to inflammatory cytokines (e.g. IL-12). Effector CD8 T cells that are exposed to lower levels of inflammation express less T-bet (light blue cells) and begin to upregulate IL-7R to become KLRG1$^{lo}$ IL-7R$^{hi}$ MPECs (turquoise cells). Effector CD8 T cells that encounter higher levels of inflammatory cytokines express relatively more T-bet and KLRG1 (dark blue cells), stably repress IL-7R and consequentially become KLRG1$^{hi}$ IL-7R$^{lo}$ SLECs. SLECs become IL-15 dependent, however, IL-15 alone cannot support their long-term persistence or homeostatic turnover and they decline over time. In contrast, MPECs remain dually responsive to IL-7 and IL-15 and preferentially develop into long-lived memory CD8 T cells that can self-renew.

UPMC PARIS UNIVERSITAS

B. Bellier

# Différenciation dès la 1ere division

**Asymmetric T Lymphocyte Division in the Initiation of Adaptive Immune Responses**
***Chang et al, Science 2007***

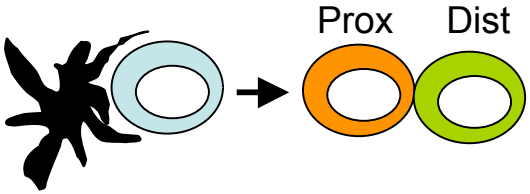


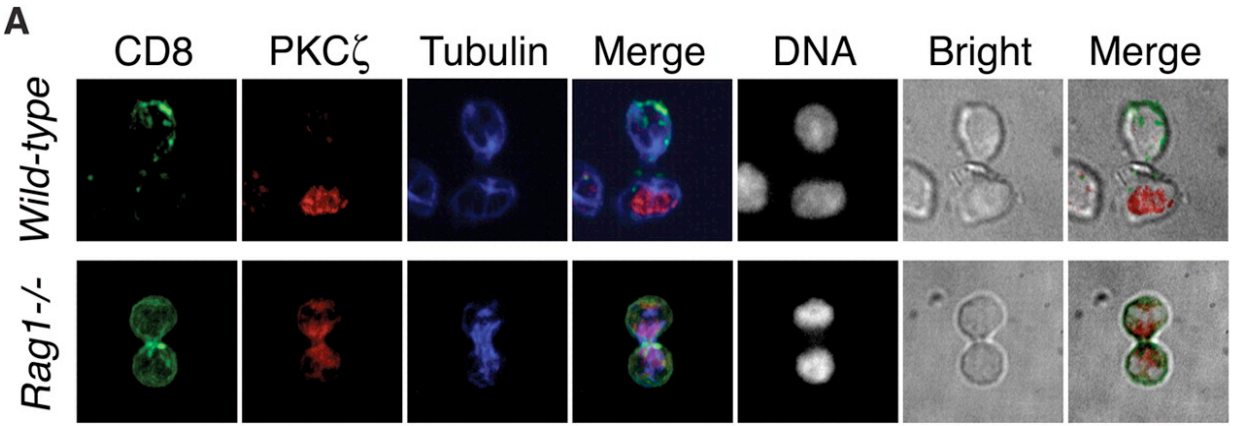


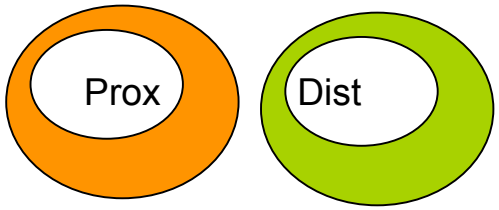


**Tbet$^{hi}$** **Prot (degrad Tbet)**

**Eff** **Mem**

*unpublished*

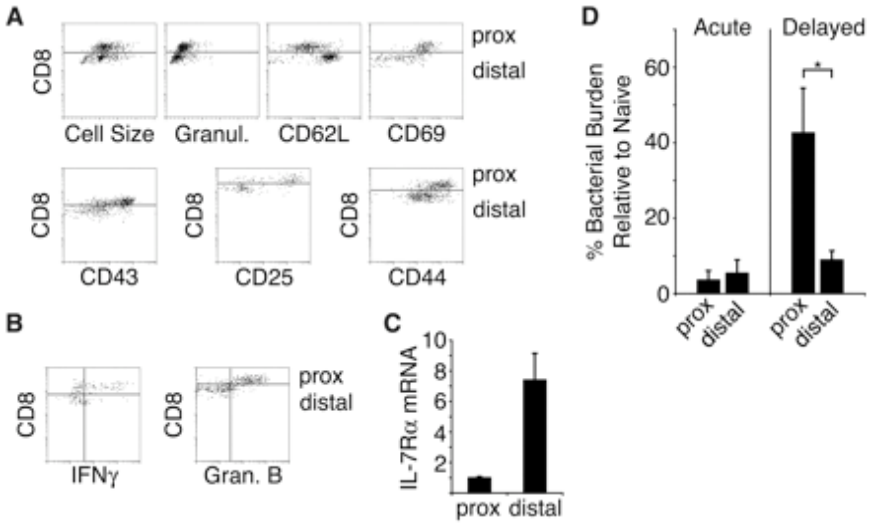

# Conclusions

- Paramètres de l'interaction TCR/CMH-Ag
  - **Affinité**
  - **Avidité**
  - **Temps contact**
  - **Flexibilité du CMH-Ag**
  - **Molécules adaptatrices / costimulation**

- Déterminent
  - **Activation lymphocytaire**
  - **Différenciation lymphocytaire**